

**DESIGN AND SIMULATION OF HYBRID PIEZO-  
PYROELECTRIC ENERGY CONVERSION DEVICE**

**NURUL ADINA BINTI AZMAN**

**RESEARCH PROJECT SUBMITTED IN PARTIALLY  
FULFILMENT OF THE REQUIREMENTS FOR THE  
DEGREE OF MASTER OF MECHANICAL  
ENGINEERING**

**FACULTY OF ENGINEERING  
UNIVERSITY OF MALAYA  
KUALA LUMPUR**

**2021**

**UNIVERSITY OF MALAYA**  
**ORIGINAL LITERARY WORK DECLARATION**

Name of Candidate: Nurul Adina Binti Azman

Matric No: S2011034

Name of Degree: Master of Mechanical Engineering

Title of Research Report (“this Work”): Design and Simulation of Hybrid Piezo-pyroelectric Energy Conversion Device

Field of Study: Vibration and Heating

I do solemnly and sincerely declare that:

- (1) I am the sole author/writer of this Work;
- (2) This Work is original;
- (3) Any use of any work in which copyright exists was done by way of fair dealing and for permitted purposes and any excerpt or extract from, or reference to or reproduction of any copyright work has been disclosed expressly and sufficiently and the title of the Work and its authorship have been acknowledged in this Work;
- (4) I do not have any actual knowledge nor do I ought reasonably to know that the making of this work constitutes an infringement of any copyright work;
- (5) I hereby assign all and every rights in the copyright to this Work to the University of Malaya (“UM”), who henceforth shall be owner of the copyright in this Work and that any reproduction or use in any form or by any means whatsoever is prohibited without the written consent of UM having been first had and obtained;
- (6) I am fully aware that if in the course of making this Work, I have infringed any copyright whether intentionally or otherwise, I may be subject to legal action or any other action as may be determined by UM.

Candidate’s Signature

Date: 30/08/2021

Subscribed and solemnly declared before,

Witness’s Signature

Date: 02/09/2021

Name: Dr Mohd Nashrul Bin Mohd Zubir

Designation: Senior Lecturer

# **DESIGN AND SIMULATION OF HYBRID PIEZO-PYROELECTRIC ENERGY CONVERSION DEVICE**

## **ABSTRACT**

Sustainable energy had been eye as a huge opportunity to replace current fossil energy since it can be harvest in various forms. This study focusing on piezoelectric energy and pyroelectric energy which involves heating and vibration energy sources considering it is common phenomenon produce by numerous mechanical systems for example car engine and HVAC system. This study aims to design and simulate the performance of hybrid piezo-pyroelectric energy for low grade applications. The design of the hybrid piezo-pyroelectric conversion device is done by using SolidWorks. This study introduces performance of the device when different air heat temperature and force by air flow release from condenser is applied to the device. ANSYS is used for analytical calculation to compare the result with theoretical calculation. Both analytical and theoretical power output produce is compared. This study proved that force and heat temperature does affect the power output and voltage output of the device. From the results, it shows that analytical calculation value is higher than theoretical calculation for voltage output and total power output for both air heat temperature and force by air flows parameter. The result shows the tendency of air heat temperature produce higher voltage output and total power output than force by air flow release.

**Keywords:** Heating, vibration, hybrid piezo-pyroelectric energy, temperature, force.

# **REKA BENTUK DAN SIMULASI PERANTI PENUKARAN TENAGA**

## **HIBRID PIEZO-PIROELEKTRIK**

### **ABSTRAK**

Tenaga lestari dianggap sebagai peluang besar untuk menggantikan tenaga fosil semasa kerana ia dapat dituai dalam pelbagai bentuk. Kajian ini memfokuskan pada tenaga piezoelektrik dan tenaga piroelektrik yang melibatkan sumber tenaga pemanasan dan getaran memandangkan ini adalah fenomena yang banyak dihasilkan oleh sistem mekanikal seperti enjin kereta dan sistem HVAC. Kajian ini bertujuan untuk merancang dan mensimulasikan prestasi tenaga hibrid piezo-piroelektrik hibrid untuk aplikasi kelas rendah. Reka bentuk peranti penukaran hybrid piezo-piroelektrik dilakukan dengan menggunakan perisian SolidWorks. Kajian ini memperkenalkan prestasi peranti apabila suhu dan daya panas yang berbeza dari aliran udara dari kondenser dihalakan pada peranti. ANSYS digunakan untuk pengiraan analitik untuk membandingkan hasilnya dengan pengiraan teori. Kedua-dua hasil output daya analitik dan teori dibandingkan. Kajian ini membuktikan bahawa daya dan suhu mempengaruhi output kuasa dan output voltan peranti. Dari hasilnya, ini menunjukkan bahawa nilai pengiraan analitik lebih tinggi daripada pengiraan teoritis untuk output voltan dan jumlah output daya untuk kedua-dua suhu panas udara dan parameter daya oleh aliran udara. Hasilnya menunjukkan kecenderungan suhu haba udara menghasilkan output voltan yang lebih tinggi dan jumlah output daya daripada daya oleh pembebasan aliran udara.

Keywords: suhu, daya, tenaga hybrid piezo-piroelektrik, haba, voltan

## ACKNOWLEDGEMENTS

First and foremost, praises and thanks to Allah, the Almighty, for His showers of blessings and letting me through all the difficulties throughout my research work to complete the research successfully.

I would like to acknowledge and give my warmest thanks to my supervisor Profesor Madya Ir Dr Mohd Faizul Bin Mohd Sabri who made this work possible. His guidance and advice carried me through all the stages of writing my project. His support given throughout the duration of this project has made me succeed to finish this research project.

I would also like to give special thanks to my parents, En Azman and Puan Asila, without you none of this would indeed be possible. Last but not least, I express my thanksto all my family as a whole for their continuous support and understanding when undertaking my research and writing my project. Your prayer for me was what sustained nethis far.

## TABLE OF CONTENTS

Abstract .....	iii
Abstrak .....	iv
Acknowledgements .....	v
Table of Contents .....	vi
List of Figures .....	ix
List of Tables.....	xii
List of Symbols and Abbreviations.....	xiii
List of Appendices .....	xv
<b>CHAPTER 1: INTRODUCTION.....</b>	<b>1</b>
1.1 Background of study.....	1
1.2 Problem Statement.....	2
1.3 Objective of the study .....	3
1.4 Relevance of study.....	4
1.5 Scope and limitation of study .....	4
1.6 Organization of the thesis .....	5
<b>CHAPTER 2: LITERATURE REVIEW.....</b>	<b>6</b>
2.1 Introduction.....	6
2.2 Piezoelectric energy.....	6
2.3 Piezoelectric material.....	10
2.3.1 Piezoelectric energy system .....	12
2.4 Transducer design.....	13
2.5 Mode generators .....	17
2.6 Pyroelectric energy .....	19

2.6.1	Concept of pyroelectricity .....	22
2.7	Piezoelectric and pyroelectric effect on PVDF material .....	26
2.8	Hybrid Piezo-pyroelectric system.....	28
2.10	Summary of previous research device .....	30
<b>CHAPTER 3: METHODOLOGY .....</b>		<b>33</b>
3.1	Methodology .....	33
3.2	Flowchart .....	33
3.3	Selection of Material.....	34
3.4	CAD design .....	36
3.5	Multiphysics modeling method .....	37
3.5.1	Direct coupled-field elements.....	37
3.6	Design consideration .....	37
3.6.1	Theoretical calculation .....	40
3.7	Design of hybrid piezo-pyroelectric device.....	42
3.7.1	Device design .....	44
3.8	Simulation.....	47
3.8.1	Engineering data.....	48
3.8.2	Geometry .....	49
3.8.3	Modeling .....	49
3.8.4	Setup.....	50
3.8.5	Analysis .....	51
<b>CHAPTER 4: RESULTS &amp; DISCUSSION.....</b>		<b>53</b>
4.1	Introduction.....	53
4.2	Results .....	54
4.2.1	Effect of heat temperature difference on power performance.....	55

4.2.2	Effect of different force applied on power performance .....	59
4.2.3	Effect of different HDPE length on power performance.....	63
4.2.4	Effect of different HDPE thickness on power performance.....	64
4.3	Discussion.....	66
<b>CHAPTER 5: CONCLUSION &amp; RECOMMENDATION.....</b>		<b>70</b>
5.1	Conclusion .....	70
5.2	Recommendation .....	71
References.....		73
Appendices.....		76

Universiti Malaysia

## LIST OF FIGURES

Figure 2.1: Monocrystal .....	8
Figure 2.2: Polycrystal .....	8
Figure 2.3 (a): Polarizations .....	9
Figure 2.3 (b): Surviving Polarity .....	9
Figure 2.4: Relationship between piezoelectric, pyroelectric, and ferroelectric materials in crystal class .....	10
Figure 2.5: Three phases related to piezoelectric energy harvesting .....	13
Figure 2.6: Cantilever beam transducer .....	15
Figure 2.7: Unimorph and bimorph piezoelectric device arrangement.....	15
Figure 2.8: Circular diaphragm transducer (a) Front view (b) Side view .....	15
Figure 2.9: Cymbal transducer .....	16
Figure 2.10: Stack piezoelectric transducer .....	16
Figure 2.11: Rectangular cantilever beam.....	17
Figure 2.12: $d_{31}$ mode of operation .....	18
Figure 2.13: $d_{33}$ mode of operation .....	19
Figure 2.14: Pyroelectric effect.....	21
Figure 2.15: Origin of the pyroelectric current is depicted in a schematic drawing .....	22
Figure 2.16: Properties of crystal that occur during thermodynamic reversible interactions respectively thermal, mechanical, and electrical .....	24
Figure 2.17: Pyroelectricity is depicted schematically in two dimensions .....	26
Figure 3.1: Flowchart of the project.....	34
Figure 3.2: Discipline in CAD design.....	36
Figure 3.3: Dimension for air-conditioner condenser .....	39

Figure 3.4: Illustration of parallel (a) and series (b) connection in bimorph .....	43
Figure 3.5: Schematic diagram of energy harvester and cross-sectional view of bimorph .....	43
Figure 3.6: Isometric view for the device position .....	44
Figure 3.7: Isometric view details of the device mounting structure.....	45
Figure 3.8: Details of cantilever configuration .....	45
Figure 3.9: Isometric view of cantilever configuration.....	46
Figure 3.10: Cantilever design dimension .....	46
Figure 3.11: Flowchart of simulation.....	48
Figure 3.12: Geometry of hybrid piezo-pyroelectric .....	49
Figure 3.13: Meshing for piezoelectric .....	49
Figure 3.14: Fixed support of the device .....	51
Figure 3.15: Analysis system of hybrid simulation .....	52
Figure 4.1: Deformation during frequency 115.13 Hz.....	53
Figure 4.2: Deformation during frequency 1649.1 Hz.....	54
Figure 4.3: Deformation during frequency 1909.1 Hz.....	54
Figure 4.4: Deformation during frequency 2490.5 Hz.....	54
Figure 4.5: Heat temperature displacement.....	55
Figure 4.6: Stress produce for heat temperature difference .....	56
Figure 4.7: Voltage output of heat temperature difference .....	56
Figure 4.8: Power output when different heat temperature applied on bottom PVDF ...	57
Figure 4.9: Force displacement.....	60
Figure 4.10: Stress produce for different force applied .....	60
Figure 4.11: Voltage output of force difference.....	61

Figure 4.12: Power output when different force is applied.....	61
Figure 4.13: Power output on different HDPE length.....	63
Figure 4.14: Total deformation 4 .....	64
Figure 4.15: Total deformation 10 .....	64
Figure 4.16: Power output on different HDPE thickness.....	65
Figure 4.17: Total deformation 7 .....	65
Figure 4.18: Total deformation 8 .....	66

Universiti Malaya

## LIST OF TABLES

Table 2.1: Comparison between PZT and PVDF.....	12
Table 2.2: Equations for pyroelectrics and piezoelectric .....	29
Table 2.3: Summary of previous research on piezoelectric material and configuration.....	30
Table 3.1: Generated peak power for piezoelectric materials .....	35
Table 3.2: Specifications of Goodman Air Conditioner Condenser with Heat Pump ....	39
Table 3.3: Parameter of the design.....	40
Table 3.4: Parameter used for theoretical calculation .....	40
Table 3.5: Theoretical calculation for heat temperature difference .....	42
Table 3.6: Theoretical calculation for force difference.....	42
Table 3.7: Material properties for copper, PVDF and HDPE .....	48
Table 3.8: No of elements and nodes .....	50
Table 3.9: Parameter used in setup.....	50
Table 4.1: Piezoelectric power, pyroelectric power and total power output.....	57
Table 4.2: Difference theoretical and analytical power output .....	58
Table 4.3: Difference theoretical and analytical voltage output .....	58
Table 4.4: Piezoelectric power, pyroelectric power and the total power output.....	61
Table 4.5: Difference theoretical and analytical power output .....	62
Table 4.6: Difference theoretical and analytical voltage output .....	62
Table 5.1: Number of devices needed.....	71

## LIST OF SYMBOLS AND ABBREVIATIONS

PVDF	:	Polyvinylidene fluoride
HDPE	:	High density polyethylene
d33	:	Piezoelectric strain mode d33
AC	:	Alternating current
S	:	Strain
T	:	Stress
E	:	Electric field
D	:	Charge density / electric displacement
$c_E$	:	Stiffness coefficient
$\epsilon^T$	:	Dielectric permittivity
$\epsilon_T$	:	Stress permittivity
$e$	:	Stress-charge form
$s_E$	:	Compliance coefficients
$d^T$	:	Piezoelectric coupling coefficient
$d$	:	Strain-charge form
PZT	:	Lead zirconate titanate
MFC	:	micro-fiber composites
d31	:	Piezoelectric strain mode d31
d15	:	Piezoelectric strain mode d15
$S_1$	:	Mechanical strain
$T_1$	:	Mechanical stress
$D_3$	:	Displacement/electric charge density
$s^{E}_{11}$	:	Elastic compliance in a constant electric field
$\epsilon^T_{33}$	:	Dielectric constant of the piezoelectric material under constant stress
$P_s$	:	Spontaneous polarization
PEH	:	Piezoelectric energy harvesting
PE	:	Pyroelectric effect
$\Delta T$	:	Temperature change
$\Delta P$	:	Electric polarization
$\gamma$	:	Constant-stress pyroelectric coefficient
$\Delta Q$	:	Charges generated on the crystal surface
S	:	Crystal's surface
$\epsilon^\sigma$	:	Strain- stress
$\sigma$	:	Stress
$I_p$	:	Pyroelectric current
$\rho$	:	Resistivity
PyEH	:	Pyroelectric energy harvesting
PMN-PT	:	Lead magnesium niobate-lead titanate
PLZT	:	Lead zirconate titanate
PVDF-TrFE	:	Polyvinylidene fluoride-co-trifluoroethylene
A	:	Area of material
$d_{ij}$	:	Direction of polarization
TEC	:	Thermoelectric cooler

V : Voltage  
h : Thickness of PVDF  
i : Current  
PDMS-CNTs : Polydimethylsiloxane-carbon nanotube

Universiti Malaya

## List of Appendices

Appendix A:	
Voltage output at temperature difference of $\Delta 16\text{K}$	73
Piezo impedance plot at $\Delta 16\text{K}$	73
Voltage produces at temperature difference of $\Delta 18\text{K}$	73
Piezo impedance plot at $\Delta 18\text{K}$	74

Universiti Malaya

# CHAPTER 1

## INTRODUCTION

### 1.1 Background of study

Due to excessive usage of fossil energy sources, sustainable energy had seen as an ideal replacement as in the future, these fossil energy sources will be depleted. Sustainable energy is known replenished energy that will not expired or depleted. Different kind of energy can be harvest from physical environment for example solar energy, wind energy, thermal energy, kinetic energy, vibrational energy also known as ambient energy sources (Shashank, Harisha et al. 2018). Nevertheless, piezo-pyroelectric energy had been seen as the good solution for the replacement of wind and solar energy since it can be harvest from vibrational energy and thermal energy. This study concerns about the energy harvested system for piezo-pyroelectric energy. (Koyuncuoglu, Özyurt et al. 2013) indicated that piezoelectric energy is harvested from external vibration. (Yildiz, Dakeev et al. 2015) contested that piezoelectric energy as method that translates by stressing the piezoelectric material, piezoelectric energy harvesting technology turns mechanical energy into electrical energy. When stress is applied, an electric field is produces when a piezoelectric material is stressed or deformed, charge separation occurs across the device, resulting in a voltage drop proportionate to the applied stress. Resonance makes the power output obtained is the highest especially when the harvester's natural frequency matched with the external vibration (Koyuncuoglu, Özyurt et al. 2013). (Thakre, Kumar et al. 2019) contended that a phenomenon on which when heat temperature fluctuations that converted into electrical energy is known as pyroelectricity energy. A dynamic scenario in which the heat temperature swings over time is referred to as "temperature fluctuation." As a result, this research was carried out in order to build and simulate an energy conversion device for hybrid piezo-pyroelectric energy.

One of previous study involved hybrid piezo-pyroelectric energy is by (Koyuncuoglu et al., 2013). This study using aluminium as cantilever as PZT ceramic as piezoelectric material. Under external vibration, cantilever moves between two surfaces with different temperatures. PZT ceramic exhibits both piezoelectric and pyroelectric properties. Shaker vibrates cantilever under low frequencies of 6 Hz, 8 Hz and 10 Hz. Temperature difference applied is between 0°C to 55°C. Firstly, cantilever is test using shaker only, then thermoelectric cooler (TEC) modules turned on and output voltage is observed. As concluded, when 50°C is applied, RMS voltage produce increased by 10% after hybrid piezo-pyroelectric effects is combined.

Other than that, other previous study involved hybrid piezo-pyroelectric effect by (Hu & Tao, 2016). Three experiment is conducted to study pure piezoelectric effect, pure pyroelectric effect, and hybrid piezo-pyroelectric effect. To test pure piezoelectric effect, mechanical loading with a weight of 31.7g is applied under different temperature of 35°C and 40°C. Pure pyroelectric effect is test by heated the PVDF sample until 60°C and cool it down until room temperature of 30°C and no mechanical loading was applied. For hybrid piezo-pyroelectric effect, PVDF sample is heated until 60°C and cool it down until 30°C and mechanical loading was applied during cooling stage. Based on the findings, it concluded that hybrid piezo-pyroelectric effect equivalent to sum of pure piezoelectric effect and pure pyroelectric effect.

## **1.2 Problem statement**

Definition of energy harvesting is the process of converting energy tapped from physical environment into useful electrical energy accorded to (Shashank et al., 2018). Waste heat and vibration energy must be harvested for useable uses in order to increase primary energy consumption efficiency, as this energy is renewable. Besides that, the source to harvest the energy also easy to acquire as many mechanical systems release hot

and cold wind. This energy which is known as piezo-pyroelectric energy as involved both vibration and heating or cooling at the same time. This energy was seen as one of the ideal replacements for primary energy. A lot of research has been done to harvest this energy as a replacement to current energy. In the past ten years, this energy has been studied and a lot of methods have been tried to harvest this energy since researchers see a huge potential in this energy. However, there is a limitation in this energy. It produces very small values of energy.

Nevertheless, a lot of current research has been done to improve the limitation and increase the power output and voltage output produced from the energy harvesting device in order to harvest more power output. Countless experiments have been in numerous methods to harvest this energy. Besides, simulation also is done to get the performance for the configuration or device. In this study, the aim is to design a conversion device that acts as a future replacement for current sources to convert into electricity. The size and dimension of the device will determine the voltage and power output produced. To improve the power and voltage produced, the design can be improved by time. Other than that, this study aims to explore the performance of the hybrid piezo-pyroelectric energy scavenging device. It will calculate the voltage and power output generated from the conversion device by using different parameters of force and heat temperature applied to the device.

### **1.3 Objective of the study**

The main objective of this study is to design the energy hybrid conversion device that can be used for low heat grade applications. This device can be used to power up sensors to save energy. In this study, sustainable energy is harvested as a replacement to primary sources. In this research, other specific objectives need to be achieved are as follows:

- 1) To design a hybrid piezo-pyroelectric energy scavenging device for low heat grade applications

- 2) To perform theoretical and analytical calculation of the power output
- 3) To model and simulate the performance of the hybrid piezo-pyroelectric energy scavenging device

#### **1.4 Relevance of study**

As a significant, this study was conducted to help produce sustainable energy from heat waste and vibration energy since the primary energy utilization will be depleted, so sustainable energy was needed as replacement. In this study, the energy harvest involving two energy sources and two different type of energy harvesting. Force and heat temperature parameter are the main highlight of this study. Comparison between these two parameters is made to see which one produce higher power output and voltage output. This can help to produce more power for energy harvesting purposes. Thus, more sustainable energy can be harvested to power up more device.

#### **1.5 Scope and limitation of study**

This study focuses on energy harvesting from heating and vibration when different parameter of force and temperature is applied to the device. In this study, it covers on  $d_{33}$  conversion mode of piezoelectric energy harvester. PVDF is used as the piezoelectric material and copper is used as electrode and HDPE is used as cantilever beam. The elasticity of the HDPE to produce higher piezo-pyroelectricity are tested. Hybrid conversion device is design by using SolidWorks and the performance of the device is simulated using ANSYS. The power output and voltage output of the hybrid conversion device produce generate from the simulation.

## 1.6 Organization of the thesis

Chapter 1 represents the introduction of this study which consists of problem statement, objectives, relevance, and scope of study. Chapter 2 discusses about the literature review of the piezoelectric energy, pyroelectric energy, hybrid piezo-pyroelectric energy system, piezoelectric material, mode generator of the configuration as well as transducer design. Chapter 3 reported about the design of hybrid piezo-pyroelectric conversion device and the simulation setup. This chapter discussing about the parameter used for this study. Other than that, chapter 4 discussing about the result produce for the simulation which is the displacement, voltage output and power output. This chapter also discusses about effect of HDPE dimension on power output produce. Lastly, chapter 5 concludes all the works in this study and discussing about future recommendation to improve current study.

## CHAPTER 2

### LITERATURE REVIEW

#### 2.1 Introduction

Energy harvesting is an important part of exploring alternate energy alternatives to conventional power sources for small and low-power electronic gadgets in the current era of global energy crises. Energy harvesting, also known as energy scavenging, defined as the technique gaining or harvest certain quantity of energy from a variety of sources, including ambient light, ambient radio frequency, thermal, and mechanical energy. Moving from conventional sources such as fossil energy to non-traditional sources such as wind, solar, piezoelectric, pyroelectric, and others requires justification. As a result, mechanical energy is referred to as the most versatile energy because it is found everywhere and is easily turned into useful electric energy (Sezer & Koç, 2021). The piezoelectric effect is the best method for capturing ambient mechanical energy since it is independent of the material's inherent polarization (Sezer & Koç, 2021). It is defined as a direct effect from a reversible process which exhibits the internal generation of electrical charges resulting from an applied mechanical force and its reverse effect which is when an electric field is applied and form internal generation of a mechanical strain (Arevalo Carreno & Foulds, 2013).

#### 2.2 Piezoelectric energy

Since piezoelectric has been a hot topic for years due to its immense potential for energy production, researchers have been looking into ways for energy harvesting and scavenging. Mechanical vibration can be used to recover energy, according to (Xie, Mane et al. 2010). Due to easy process to extract energy from the surrounding system into electrical energy, piezoelectric had been focusing and explore as potential replacement energy. (Yildiz, Dakeev et al. 2015) indicated that squeezing and pressing as piezoelectric

definition. (Hu and Tao 2016) mentioned piezoelectric energy converts mechanical deformation into electricity. (E and Rajakumar 2018) mentioned that a weak electrical output was produced by converting mechanical strain of piezoelectric elements. Direct and reverse effects are the two types of piezoelectric effects. The mechanical strains that generate electrical charge are known as the direct effect, whereas converse effect defined as applications of an electric field that generate mechanical movement. In piezoelectric energy harvest, the direct effect is used as the piezoelectric is harvested by external vibration. Thus, it proves that mechanical stress is used during harvesting the energy. The process of piezoelectric energy harvesting involves straining a piezoelectric material to convert mechanical energy to electrical energy (Yildiz et al., 2015). An electric field is created when a piezoelectric material is stretched or deformed, causing charge separation across the device and a voltage drop proportionate to the applied stress. On ceramics with piezoelectric characteristics on their polar axis, mechanical stress generates voltage (Koyuncuoglu et al., 2013). When resonance occurs, external vibration frequency that matches the harvester's inherent frequency can provide the highest power production. Piezoelectric materials able to convert mechanical energy deformation into electricity (Hu and Tao 2016). Furthermore, piezoelectricity may be used to generate electric potential in components such as crystals and some types of ceramics due to mechanical stress. Mechanical strain turns into electrical current and voltage from the piezoelectric effect obtain due to underlying structure of a crystal lattice. Due to the charge balance of negative and positive polarization in certain crystalline formations, neutralization is done along the imaginary polar axis. The energy is then transferred onto the crystal mesh by the electric charge when there is a balance issue with external tension, which creates current inside the crystal. Furthermore, unbalance neutral charge state happens due to generated mechanical tension from piezoelectric effect obtains from an external charge input. The polar axes of all charge carriers in a monocrystal, on the other hand, have one-

way directional properties (Cali, Rongala et al. 2014). Even if the crystal was broken into pieces, the polar axes would remain unidirectional. Figure 2.1 shows monocrystal illustrations.

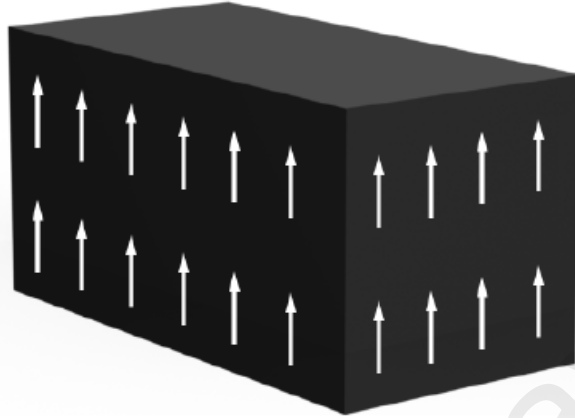


**Figure 2.1 : Monocrystal (Caliò et al., 2014)**

Varying sections inside a material with different polar axes are known as polycrystals (figure 2.2). Since no two leftover parts would be inside the same resultant polar axes, this crystalline is asymmetrical. The polycrystal is heated to curie point while being subjected to a high electric field to achieve the piezoelectric effect. When molecules are heated, they are free to move around, and rearrange subsequently with the external from the electric field which cause it to dipole (Caliò, Rongala et al. 2014) as in figure 2.3.

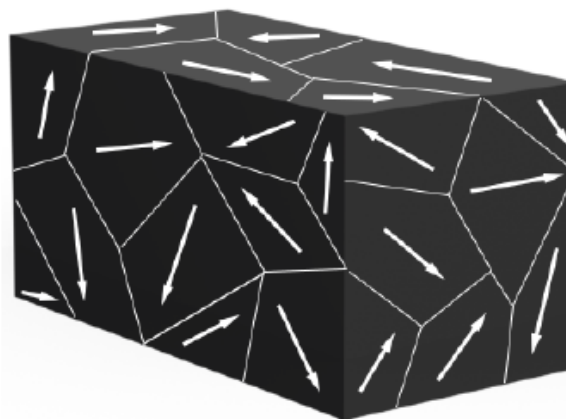


**Figure 2.2 : Polycrystal (Caliò et al., 2014)**

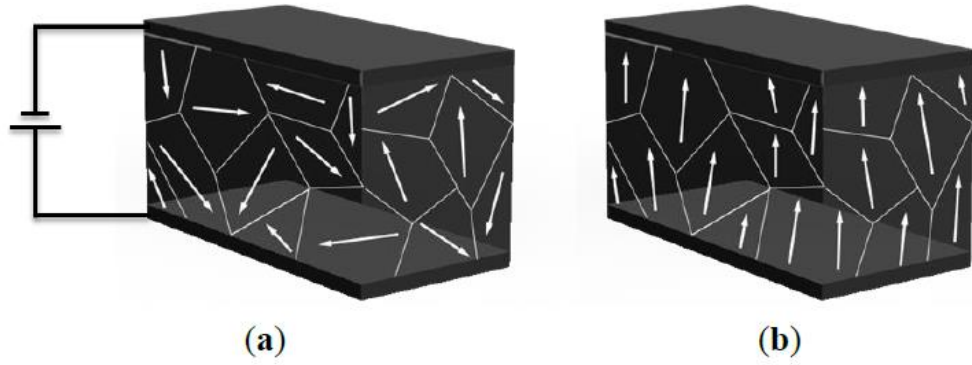


**Figure 2.3 (a) Polarizations (b) Surviving Polarity (Caliò et al., 2014)**

When the material is stretched, voltage with opposite polarity arise between them. Reversely during compression of the material, poling voltage are same like polarity of the voltage occurs in the middle of electrodes (Caliò et al., 2014). Vibration of the material occurs at the same frequency simultaneously as the signal as deformation occurs when AC signal were adapted. (Caliò et al., 2014) stated that the piezoelectric become stabilize as the properties change logarithmically with age.

Piezoelectricity has been defined as interaction between mechanics and electric fields of a structures (Arevalo Carreno & Foulds, 2013). By using electric constants, the coupling of linear elasticity equations and electrostatic charge equations has been modelled as the interaction of piezoelectricity. Thus, the stress-charge equation can be expressed in constitutive form:

$$T = c_E S - e^T E \quad (2.1)$$

$$D = e S - \varepsilon_T E \quad (2.2)$$

Where S is defined as strain, T is stress, E is electric field and D is the charge density displacement interact between them. Thus, the strain charge constitutive form can be expressed as:

$$S = s_E T - d^T E \quad (2.3)$$

$$D = d T - \varepsilon_T E \quad (2.4)$$

### 2.3 Piezoelectric material

Set of parameters can describe each piezoelectric material. When stress is taken into account as an input, the strain coefficient creates a link between applied stress and electric induction (Caliò et al., 2014). A high energy density piezoelectric material produced a massive strain coefficient and voltage constant product. Combining mechanical and electrical properties of material with piezoelectric capabilities can produce harvested energy converter and its efficiency. The mechanical characteristic of Young's modulus describe the device's resilience and toughness (Caliò et al., 2014). Furthermore, it is crucial in determining piezoelectric coefficients, coupling factor, and dielectric permittivity. All these material-dependent properties are critical in the design of a harvesting system, and material selection is one of the most important factors in piezoelectric harvester material selection.

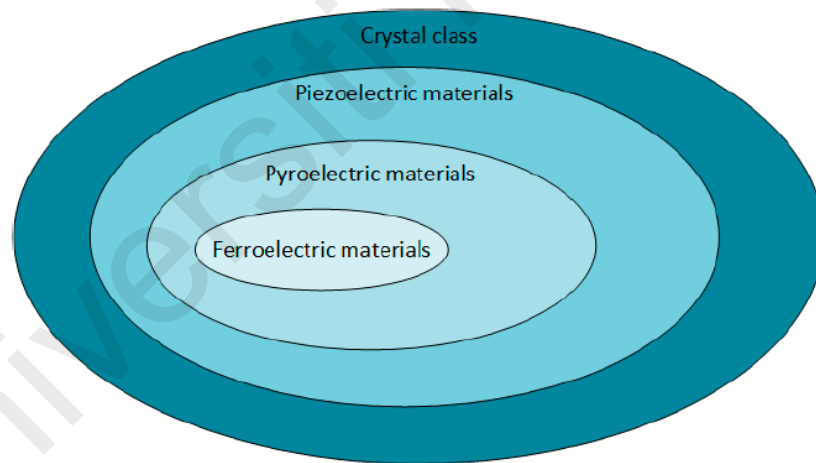


**Figure 2.4 : Relationship between piezoelectric, pyroelectric and ferroelectric materials in crystal class (Covaci & Gontean, 2020)**

According to the study (Covaci & Gontean, 2020), 20 of the 32 crystal classes have direct piezoelectricity (figure 2.4), with polar crystals constituting ten of them (exhibit spontaneous polarization in the absence mechanical stress). These polar crystals will exhibit pyroelectricity and generate a charge when exposed to an oscillating heat gradient. Several materials for harvesting piezoelectric energy have been developed. Piezoelectric

materials may also exist in nature. Quartz and bones are examples of natural piezoelectric materials; however, synthetic piezoelectric materials such as PZT and PVDF are more commonly used in engineering applications. PZT is an inorganic ceramic substance that is delicate in nature, despite having a high piezoelectric coefficient. One of the material's drawbacks is that it is poisonous. PVDF is a flexible and long-lasting polymer due to its low piezoelectric coefficient.

Piezoelectric ceramics, also known as piezoceramics, are a type of piezoelectric material that has been widely used in sensors and actuators in recent years. As eloquently stated by (Safaei et al., 2019), PZT (polycrystalline monolithic piezoelectric ceramic) is a type of polycrystalline monolithic piezoelectric ceramic that is typically doped with niobium or lanthanum to produce soft or hard piezoelectric material. Soft PZT has a power density three orders of magnitude higher than high-temperature crystals at ambient temperature, according to research by (Ghazanfarian & Mohammadi, 2021). This is due to their capacity to output high voltages on the order of 50V to 100V, as well as direct coupling, which allows them to operate without a bias voltage (Safaei et al., 2019). In their research, (Ghazanfarian & Mohammadi, 2021) mentioned that the coupling coefficients of soft ceramics are high, and the mechanical quality factors are moderate, whereas the coupling coefficients of hard ceramics are lower, and the mechanical quality factors are greater. The downsides of employing PZT include lead toxicity, which might result in health hazards (Ghazanfarian & Mohammadi, 2021).

Highly flexible materials include PVDF polymer and MFC as argued by (Caliò et al., 2014). Composite produce when flexibility of epoxy and piezoceramic material's energy density are combine is MFCs. When PZT, PCDF, and MFC are compared, PZT has the highest power density; however, due to its low yield strength, it is not suitable for high g-vibrations. Low yield strength can lead to a reduction in robustness, which can lead to fractures (Caliò et al., 2014).

Thus, piezo-materials can be concluded as an excellent material to replace batteries for powering macro and nanoscale electronic devices with short lifespan as stated in study by (Ghazanfarian & Mohammadi, 2021).

The performance of piezoelectric energy harvest depends on the piezoelectric materials. For energy harvesting, the most important criteria to be considered is output voltage, power density, operational bandwidth and functionality at working situation as studied by (Ghazanfarian & Mohammadi, 2021). Table 2.1 below shows the comparison of piezoelectric polymers (PVDF) and piezoelectric ceramics (PZT) properties/parameters.

**Table 2.1 : Comparison between PZT and PVDF (Covaci & Gontean, 2020)**

Properties/Parameters	Piezoelectric Ceramics (PZT)	Piezoelectric Polymers (PVDF)
Piezoelectricity	High	Low
Acoustic impedance ( $10^6 \text{ kg m}^{-2} \text{ s}^{-1}$ ) <sup>1</sup>	High (30)	Low (2.7)
Density ( $10^3 \text{ kg m}^{-3}$ )	7.5	1.78
Relative permittivity ( $\epsilon/\epsilon_0$ )	1200	12
Piezoelectric strain constant ( $10^{-12} \text{ C N}^{-1}$ )	$d_{31} = 110, d_{33} = 225-590$	$d_{31} = 23, d_{33} = -33$
Piezoelectric stress constant ( $10^{-3} \text{ V m N}^{-1}$ ) <sup>1</sup>	$g_{31} = 10, g_{33} = 26$	$g_{31} = 216, g_{33} = -330$
Electromechanical coupling factor <sup>2</sup>	$k_{31} = 30$	$k_{31} = 12$
Dielectric constant	1180	10-15
Mechanical flexibility <sup>1</sup>	Poor	Outstanding
Curie temperature ( $^{\circ}\text{C}$ )	386	80

<sup>1</sup> Exceptional properties of PVDF for energy harvesting application vis-à-vis PZT ceramics. <sup>2</sup> % at 1 kHz.

## 2.4 Piezoelectric energy system

In piezoelectric energy system, there are 3 phases of harvesting systems. The phases are mechanical – mechanical energy conversion, mechanical – electrical energy conversion, and electrical – electrical energy conversion as shown in figure 2.5. In phase 1, mechanical strength of piezoelectric energy was harvested under massive loads and mechanical impedance was matched, which is mechanical to mechanical energy conversion. The phase 2 entails the conversion of mechanical to electrical energy. This phase involves piezoelectric coefficients and the piezoelectric energy harvester structure's electromechanical coupling factor. When it comes to phase 3, it entails electrical impedance matching as mentioned in study by (Covaci & Gontean, 2020).

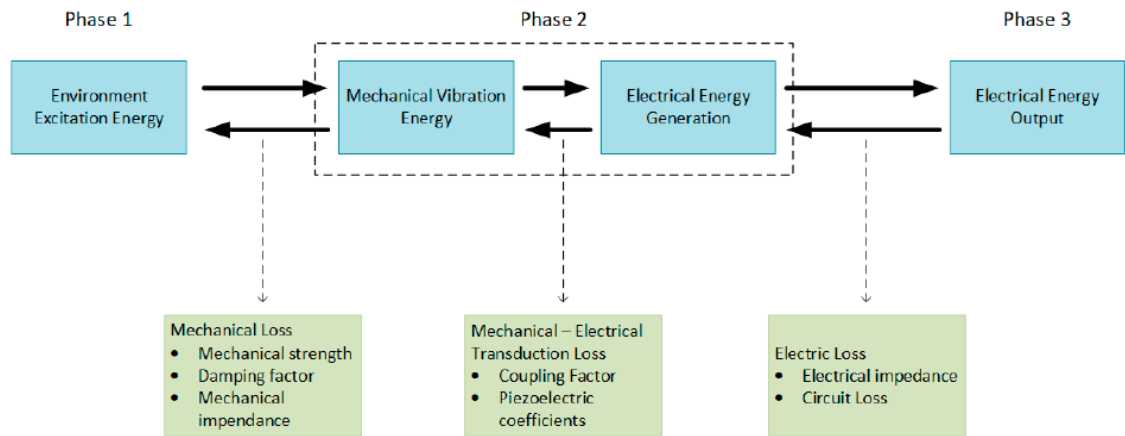


**Figure 2.5 : Three phases related to piezoelectric energy harvesting (Covaci & Gontean, 2020)**

Natural excitation mode and forced or external excitation mode are the two types of piezoelectric energy that can be harvested. Natural excitation mode is a way of feeding input mechanical force naturally and leaving the system unaffected, or externally supplied the input mechanical force that requires attention. As this mode produces very less input vibration, it is not favored. Nevertheless, external or known forced excitation mode is known as conventional method but still be used until now. This is due to the generated output produced by the forced excitation mode highly compared with natural excitation mode. Forced excitation mode is defined as a way of applying mechanical force by produce it from combining two phenomenon.

## 2.5 Transducer design

There are multiple ways can be done for piezoelectric energy harvesting. For the transducers design, it are regularly observed all through some shapes in study by (Covaci & Gontean, 2020) :

- 1) Cantilever beam
- 2) Circular diaphragm
- 3) Cymbal type

#### 4) Stack type

Based on past research, there are a few designs and arrangement had been used for piezoelectric energy harvesting. If using cantilever beam, there are two ways to implement it. Cantilever beams are widely used for piezoelectric energy harvesting because they have a simple geometry and only consist of a thin piezoelectric layer (or two layers) and a non-piezoelectric layer that is commonly fixed at one end to achieve a structure operating in its flexural mode (see figure 2.6). Layering materials in cantilevers can be classified into two which is unimorph and bimorph (see figure 2.7) and bimorph are divided into series and parallel. Unimorph configuration consists only one piezoelectric layer bonded to the metallic layer with a single active and passive layer while bimorph consists two piezoelectric layers linked to the metallic layer which has two active layers or a passive layer sandwiched between two active layers (E & Rajakumar, 2018) (Covaci & Gontean, 2020). In series bimorph, the serial connection is applied thus the polarization direction is opposite, whereas in parallel bimorph the electrically parallel connection is applied which results to polarization direction in parallel form. The presence of piezoelectric material on the beam's top or both sides distinguishes between unimorph and bimorph as stated by (Caliò et al., 2014). They were regarded as the best suitable for lower frequencies and resistance to load, but excellent performance at higher frequencies and larger loads was demonstrated since it was able to extract more power. Two piezoelectric parts in a bimorph cantilever experience opposite strain during operation and are connected in electrical series in order to boost up the output voltage. It also can be arrange in parallel arrangement so that output current can be boost (Caliò et al., 2014). To double up the electrical energy output, bimorph configuration is preferable since it does not change the device volume respectively.

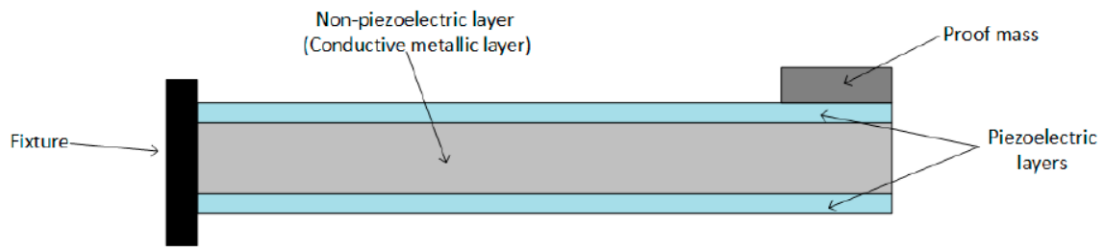


**Figure 2.6 : Cantilever beam transducer (Covaci & Gontean, 2020)**

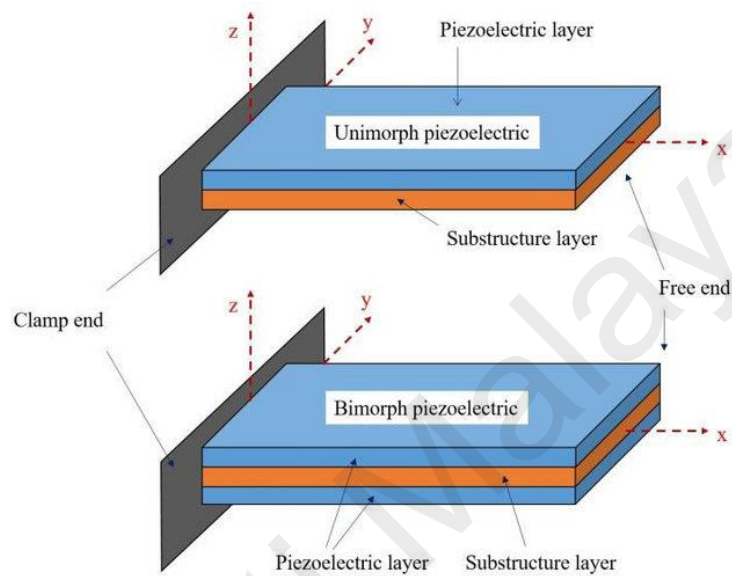


**Figure 2.7 : Unimorph and bimorph piezoelectric device arrangement (Yaakub et al., 2017)**

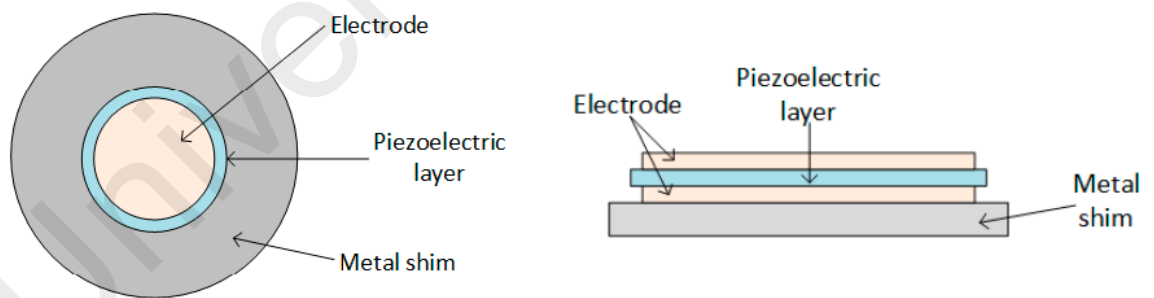


**Figure 2.8 : Circular diaphragm transducer : (a) Front view (b) Side view (Covaci & Gontean, 2020)**

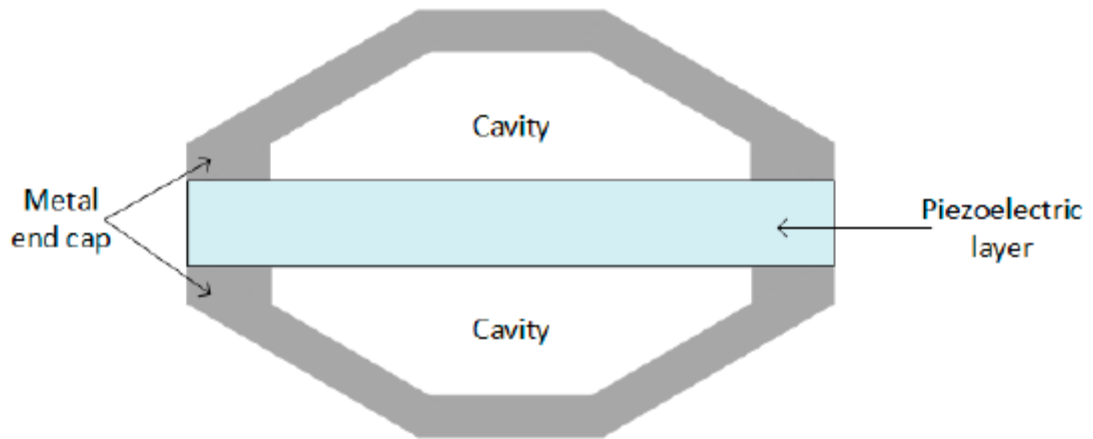


**Figure 2.9 : Cymbal transducer (Covaci & Gontean, 2020)**

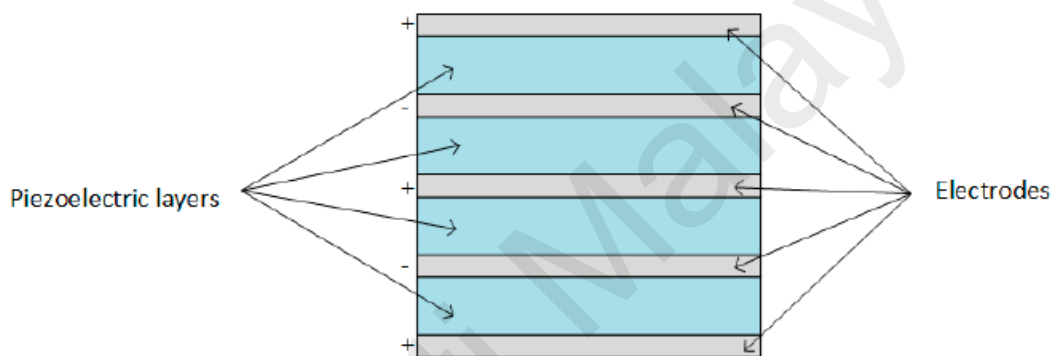


**Figure 2.10 : Stack piezoelectric transducer (Covaci & Gontean, 2020)**

Based on figure 2.8, a thin disk-shaped piezoelectric layer was used as circular diaphragm transducer and a proof mass was added to rise up the performance and power production during low frequency condition at the diaphragm's core. In figure 2.9, two metal was sandwiched at the end caps on both sides of a cymbal transducer as it gives benefit for larger impact forces scenarios. Higher charge generation from the piezoelectric energy harvester produce as a result from larger piezoelectric coefficient initiate due to axial stress applied to the metal end caps which then amplified and transfromed into radial stress in study by (Covaci & Gontean, 2020). From the illustration in figure 2.10, piled of piezoelectric layers was placed on top of each other with the layers' poling directions aligned with the applied force which then produce a stack piezoelectric transducers. For this transducer design, they are used for application which required a lot of pressure.

## 2.6 Mode Generators

The electric charge can be induced in perpendicular and parallel form to the direction of applied stress (Kim et al., 2013). There are three ways to applied stress in piezoelectric which is  $d_{15}$ ,  $d_{31}$  operating mode and  $d_{33}$  operating mode (Caliò et al., 2014) but only  $d_{31}$  and  $d_{33}$  are considered in this project since the force are applied under normal stress.  $d_{15}$  mode is usually suffering from shear stress. In  $d_{31}$  operating mode which is also known as transverse effect, the material will produce induced electric field in direction 3 in order to response to the stress along direction 1 (Caliò et al., 2014). An external electric field  $E_3$  induced the in-plane strain  $X_1$  in the piezoelectric film normal to the plane. At the end, the beam bend up when a voltage is applied to the electrodes and makes the piezoelectric film contracts laterally for  $E_3$  parallel to the remnant polarization ( $P_r$ ) of the film (Arevalo Carreno & Foulds, 2013). Figure 2.11 below shows a rectangular beam, a tip mass, and a piezoelectric material are utilized in the most common design for a piezoelectric harvester for  $d_{31}$  mode.

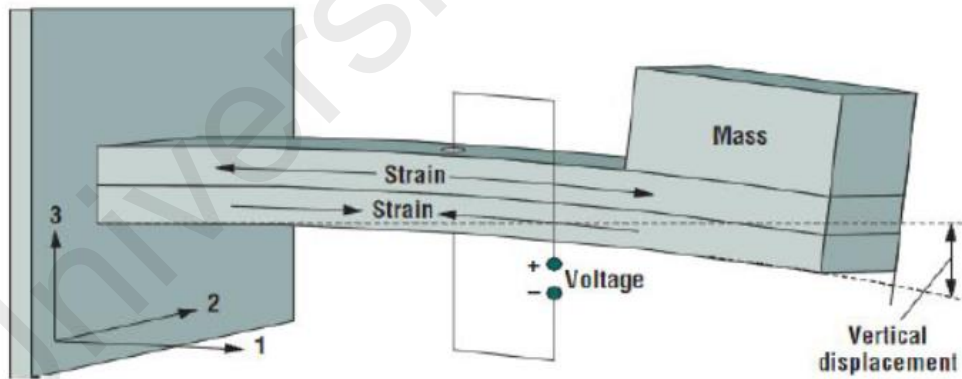


**Figure 2.11 : Rectangular cantilever beam (Caliò et al., 2014)**

For example,  $d_{31}$  mode also commonly used for two layers piezoelectric attached which known as bimorph arrangement. The equation for  $d_{31}$  mode for stress and strain can be expressed as:

$$S_1 = s_{11}^E T_1 + d_{31} E_3 \quad (2.5)$$

$$D_3 = d_{31} T_1 + \varepsilon_{33}^T E_3 \quad (2.6)$$

where  $S_1$  and  $T_1$  are the mechanical strain and stress in length direction of the piezoelectric layers.  $E_3$  is define as electric field,  $D_3$  as displacement or can be used as electric charge density.  $s_{11}^E$  is symbol for elastic compliance in a constant electric field.  $d_{31}$  is constant of piezoelectric strain and  $\epsilon_{33}^T$  is dielectric constant of the piezoelectric material under constant stress.

Based on (E & Rajakumar, 2018), the efficiency of  $d_{31}$  has been demonstrated in low vibration environments (E & Rajakumar, 2018) stated that in the  $d_{31}$  mode, a system's resonant frequency is significantly lower, causing it to drive in the natural environment at resonance, producing more power. Figure 7 below shows  $d_{31}$  mode of operation.



**Figure 2.12 : d31 mode of operation (E & Rajakumar, 2018)**

The  $d_{33}$  mode or extensional effect is defined as forces applied parallel to the polarization axis while accumulating charge perpendicular to it. The generated electric field in the  $d_{33}$  working mode will be in the same direction as the material subjected to the stress produced. In plane electric field,  $E_3$  resulting from the induced strain  $X_3$ . In  $d_{33}$  mode, the stress effect and generated voltage are in the same direction (z-axis) (Haider et al., 2020). Cantilever will bend from the transverse piezoelectric strain. This mode is crucial for enhancing the performance of the piezoelectric coefficient in research. In this operating mode, it led initially to impact harvester process. In this mode, the piezoelectric coefficient produce is higher than  $d_{31}$  mode therefore the deflection is larger in  $d_{33}$  mode and it is suitable for high vibration level sectors. In general,  $d_{33}$  mode vibrating generators are used for industrial fields for example automotive industry and machinery industry, as well as any mechanical joints involving tolerances to demonstrate the relative movements of structural components. Figure below 2.13 shows  $d_{33}$  mode of operation.

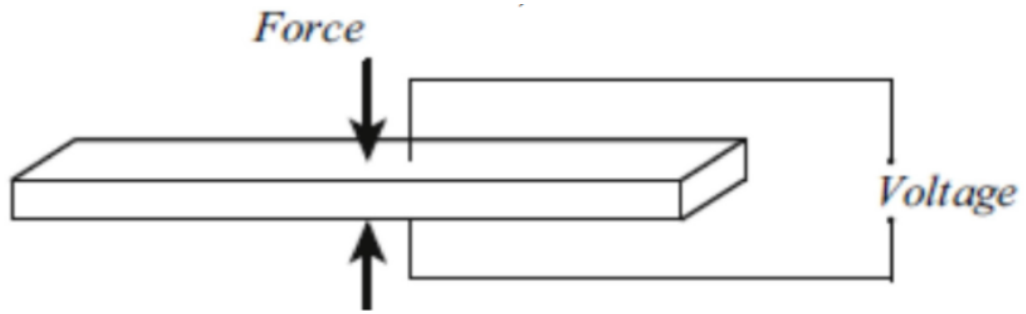


**Figure 2.13 : d<sub>33</sub> mode of operation (E & Rajakumar, 2018)**

$d_{33}$  mode produce higher voltage than in  $d_{31}$  mode and in larger current generation, it can be superior. Due to low capacitance in  $d_{33}$  mode,  $d_{31}$  were reported to give out better performance in PEH than in  $d_{33}$  mode. On the contrary,  $d_{33}$  mode exhibits better performance in device mode in actuator applications. Dead layer effect in  $d_{33}$  mode complicates the poling piezoelectric layer underneath finger electrodes (Kim et al., 2013). PEH are on the same side of piezoelectric layer for electrodes in  $d_{33}$  mode while different layers are used to stack the electrode in  $d_{31}$  mode. In consequence, for  $d_{31}$  mode, one more etching or deposition mask is required for device fabrication than in  $d_{33}$  mode. As conclusion, PEH performance strongly be influenced on the type of piezoelectric mode.

## 2.7 Pyroelectric energy

The ability to convert temperature fluctuations into usable energy is referred to as pyroelectric energy harvesting. Pyroelectricity also defined as the changes of temperature process in the environment which the convert it into electrical energy. The generation of change with a temperature change is referred to as the pyroelectric effect. The phenomena of temperature fluctuation occurs when pyroelectricity is transformed into electrical energy. Rather than harvesting energy from spatial temperature gradients, pyroelectric materials generate power from temporal temperature fluctuations (Bowen et al., 2018). In particular, when the temperature of a material changes over time, the charge is formed, in addition to temperature fluctuations that cause mechanical deformation. Temperature changes in the pyroelectric material cause charge accumulation at the electrode and

distinct application targets, resulting in the net dipole moment (Thakre et al., 2019). Pyroelectrics are non-centrosymmetric polar crystals that have an inherent relationship between electrical polarization  $P$  and temperature  $T$ , resulting in temperature variations and, as a result, a change in electric dipole moment  $PE$  (Pandya et al., 2019). As its  $PE$  manifests as a temperature-dependent change in the surface-charge density, thermally induced strain in piezoelectric materials, and flexoelectric effects from thermal gradients in all materials, PEs can also be induced by the temperature-dependence of the dielectric permittivity. Pyroelectrics are polar dielectrics that spontaneously polarize when no electric field is applied. Due to the obvious pyroelectric effect, soft pyroelectrics are common in ferroelectric polymers. Polarization in ferroelectric polymers is defined as the alignment of polarized covalent links. The polarization process results in the presence of bound charge on each surface of the material. As the temperature of the material changes, the origin of pyroelectric behavior changes, as shown in Figure 2.14 (a). As in figure 2.14 (b), due to thermal vibrations, when pyroelectric is heated at  $\frac{dT}{dt} > 0$ , the material loses its orientation, resulting in a decrease in polarization. As shown in figure 2.14, as polarization decreases, the number of free charges bonded to the material surface decreases (c). If the material is in an open circuit, the free charges remain at the electrode surface, forming an electric potential across the material. During short-circuit conditions, an electric current,  $I$  flows in between two polar surfaces of the material (Bowen et al., 2018). As in figure 2014 (b), the pyroelectric material is cooled  $\frac{dT}{dt} < 0$  which makes the material dipoles to regain its orientation. This leads to increase level of spontaneous polarization; thus, free charges are attracted to the polar surfaces now as electric current flow under short condition were reversed as in figure 2.14 (d).

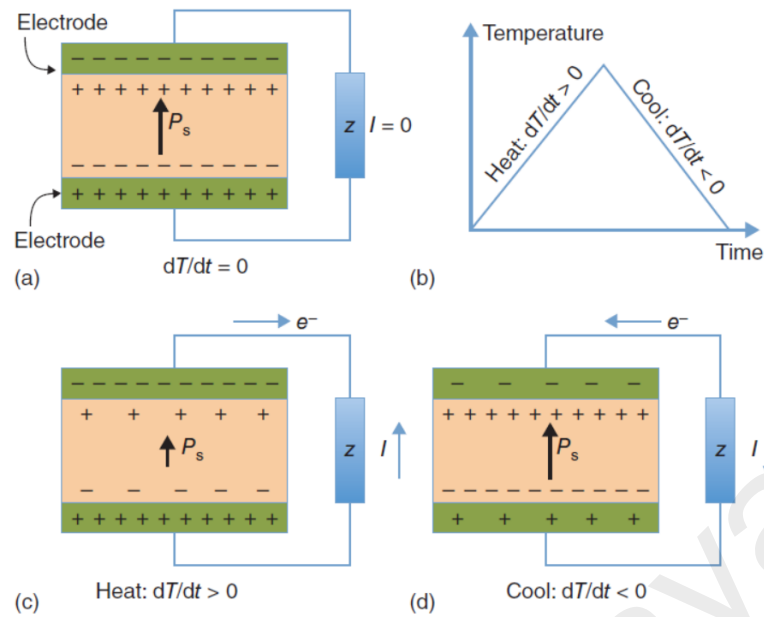


**Figure 2.14 : Pyroelectric effect (Bowen et al., 2018)**

The spontaneous polarization is denoted by  $P_s$ , while the current generated by a change in bound charge is denoted by  $I$ . Pyroelectric effect conversion (PEC) necessitates a temporal variation in temperature ( $dT/dt$ ), making it ideal for situations where temperature gradients are difficult to generate or the temperature of the heat source fluctuates (Pandya et al., 2019).

Low-grade thermal energy at low temperatures is preferable for pyroelectric energy harvesting. A thermal sensor that can detect thermal signals is an application for pyroelectric energy conversion. Thermal energy can be harvest from pyroelectric effect when total converted energy and conversion efficiency produce are high enough to charge the devices storage of electrical energy such as batteries. Furthermore, pyroelectric energy harvesters could be used to power autonomous devices. According to some studies, PEC can yield significant output power densities that can be utilized to operate devices like liquid color displays (LCD), light-emitting diodes (LED), and wireless devices.

### 2.7.1 Concept of pyroelectricity

When a temperature change,  $\Delta T$  is applied uniformly, pyroelectricity is described as certain materials exhibiting an electric polarization,  $\Delta P$ . The expression can be defined as follows:

$$\Delta P = \gamma \Delta T \quad (2.7)$$

where  $\gamma$  is the constant-stress pyroelectric coefficient. The pyroelectric effect can only be observed when the temperature of the materials changes, not during spontaneous polarization.

Pyroelectric coefficient can be expressed as:

$$\gamma = \frac{\partial P_s}{\partial T} \quad (2.8)$$

Where  $P_s$  is spontaneous polarization and the unit for pyroelectric coefficient is  $\left[\frac{C}{m^2K}\right]$  and  $T$  is the time taken for the polarization to occur.

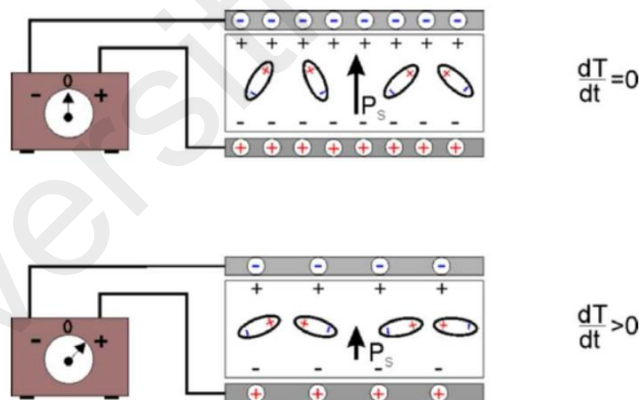


**Figure 2.15 : Origin of the pyroelectric current is depicted in a schematic drawing**

**(Triani)**

In figure 2.15 shows when  $dT/dt = 0$ , an increase in temperature,  $T$ , may stimulate spontaneous polarization,  $P_s$ , resulting in a decrease in dipole moments and a decrease in magnitude. When  $dT/dt > 0$ , the charge that builds on the crystal edge is compensated for by current flows within the materials.

The ability to generate induced charges on a crystal surface while it is being heated or cooled is referred to as pyroelectricity. Temperature changes due to the movement of positive and negative charges and the formation of electric polarization at the opposing ends of a crystal's polar axis. As an example, consider the following equation:

$$\Delta Q = \gamma S \Delta T \quad (2.9)$$

Where  $\Delta Q$  denotes the charges generated on the crystal surface and  $S$  denotes the crystal's surface.

The relationship between generated charges and polarization can be demonstrated by:

$$Q = \Delta P \cdot S \quad (2.10)$$

And the polarization unit is  $\left[ \frac{C}{m^2} \right]$

Small changes in temperature,  $\Delta T$  which is uniformly over the crystal and the polarization changes in vector,  $\Delta P$  is defined by:

$$\Delta P_i = \gamma_i \Delta T \quad (2.11)$$

where  $\gamma_i$  represents one of the three pyroelectric coefficients  $i = 1, 2, 3$ . The vector,  $\gamma$  thus specifies the pyroelectric effect in a crystal.

Pyroelectricity is depicted as one side of a triangle in Figure 2.16, with each corner representing kinetic, electrical, and thermal energy in the form of a crystal. Small changes in one of the variables will result in changes in the other variables' correlation. The lines connecting pairs of circles show these changes. The physical qualities of heat capacity, elasticity, and electrical permittivity are defined by the three short strong lines that connect pairs of thermal, elastic, and electric variables. The entropy increase,  $S$ , caused by a minor temperature increase,  $T$ , is proportional to the heat capacity divided by the temperature. Lines connecting pairs of circles in different corners of the diagram represent coupled effects and diagrams. Two contributions to the pyroelectric effect are shown as colored lines. Firstly, expansion and contraction are prevented by clamping the crystal under constant strain,  $S$ . The green line represents the primary pyroelectric effect, which

is represented by temperature variations that generate a change in electric displacement. Second, the secondary pyroelectric event caused crystal deformation. Dashed red lines shows the electric displacement alter by a strain due to piezoelectric process which caused from the thermal expansion. Although defining the primary effect can be difficult, ascertaining the secondary effect is simple using the thermal expansion coefficient, elastic stiffness, and piezoelectric strain constant quantities.

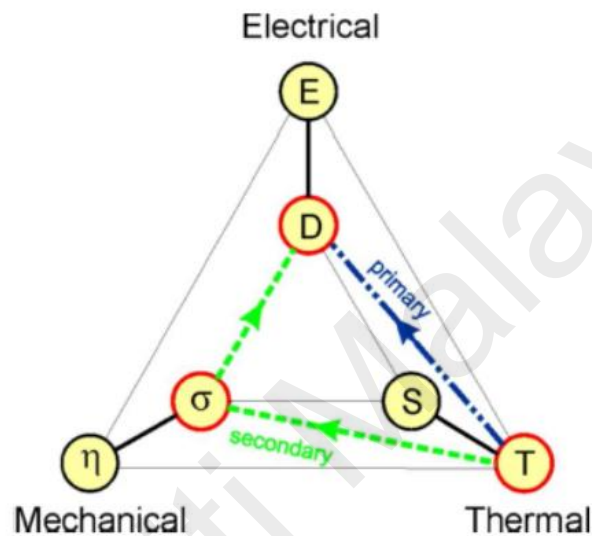


**Figure 2.16 : Properties of crystal that occur during thermodynamic reversible interactions respectively thermal, mechanical, and electrical (Triani)**

To harvest energy, pyroelectric materials require a temporal temperature gradient. A net dipole moment generated by temperature variations in the pyroelectric substance causes charge accumulation at the electrode. As a result, small microgenerators that has small dimension that can withstand temperature changes in space are separated. Separation bound charges is caused by the temperature fluctuations of pyroelectric material which led to changes in polarization. Pyroelectricity can appear in form of alternating current (AC). Pyroelectric materials with spontaneous polarization ( $P_s$ ) are a subdomain of dielectrics with polar symmetry when no electric field is applied. The crystalline structure of an ionically bound substance causes polarization. Polarization can occur in polymers due to the alignment of covalently bound atoms in the molecular chain. Transition in

polarization caused by the fluctuation in the temperature and it correlate with the electric current. When the material is heated to  $\frac{dT}{dt} > 0$ ,  $P_s$  changes, causing thermal vibration to disrupt the dipole alignment. As a result of changes in  $P_s$ , bound charge carriers tend to separate and accumulated the charges at the electrode surface. Furthermore, when the dipoles realign between them when the pyroelectric material is cooled at  $\frac{dT}{dt} < 0$ ,  $P_s$  tend to increase. All pyroelectric materials and all ferroelectrics are referred to as piezoelectric materials. This concluded that all ferroelectrics material are piezoelectric and pyroelectric. (Thakre et al., 2019) reported that piezoelectric and pyroelectric coefficients of ferroelectric materials are higher than those of non-ferroelectric materials. If ferroelectric materials are heated above their transition temperature, the properties of piezoelectric and pyroelectric materials may vanish ( $T_c$ ). It was also stated that  $P_s$  rapidly decreases after  $T_c$ . Furthermore, beyond  $T_c$ , pyroelectricity is no longer present when  $dP_s/dT$  drops to zero caused by the initial increasing until it reached  $T_c$ . Accumulated charges would be at their peak right before  $T_c$ , when the pyroelectric coefficient is at its peak.

The pyroelectric effect occurs on a microscopic scale as a result of the asymmetric interaction potential created by electrically charged atoms within the material's crystal structure. Figure 13 depicts a two-dimensional lattice of cations and anions in schematic form. Along the line ( $x_1 - x_2$ ), the electrical dipole moment or spontaneous polarisation,  $P_s$  is boosted when cations are shifted in relation to the unit cell's center.

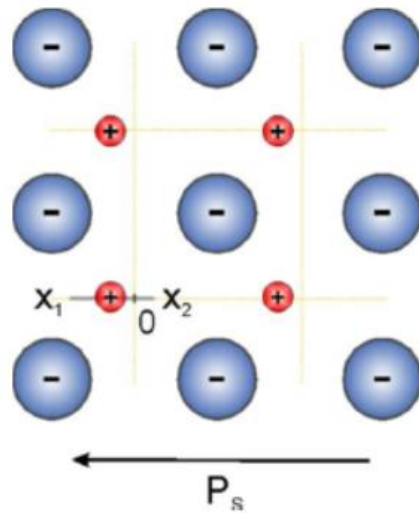


**Figure 2.17 : Pyroelectricity is depicted schematically in two dimensions (Triani)**

Along the line, the cation potential energy will be asymmetric. Changes in quantum energy levels ( $E_1$  to  $E_n$ ) within the wall are caused by increases in lattice temperature, as a result of changes in the lattice's equilibrium position along the line A-B. As a result, changes in the total electrical dipole moment. As a result of pyroelectric dielectrics, dipole moments emerge as a result of the alignment of polarized covalent bonds in molecular crystals or crystalline polymers, or as atomic displacements controlled by the location of hydrogen ions in hydrogen covalent bonds.

## 2.8 Piezoelectric and pyroelectric effect on PVDF material

PVDF is a popular material for piezo-pyroelectric materials due to its excellent flexibility, chemical resistance, thermal stability, and mechanical properties. It also has amorphous and crystalline microstructures, as well as polar and nonpolar phases. (Tao & Hu, 2016). Piezoelectric and pyroelectric effects occur when the phase conformations of the material result in net non-zero dipole moments. In order to achieve the desired content of polar crystalline phase, PVDF must be polarized in mechanical or electrical fields (Hu & Tao, 2016). PVDF is an excellent piezoelectric material when mechanical stress or deformation is applied for this orientation of the electric dipoles changes, causing charges

to accumulate on the electrode surfaces.

The direct piezoelectric action is represented by the equation below:

$$D = \varepsilon^\sigma E + d\sigma \quad (2.12)$$

Where  $D$  and  $E$  represent electric displacement and electric field, respectively, mechanical stress, dielectric permittivity in a constant stress state, and piezoelectric coefficient. The entire coupling effect between mechanical and electric fields is considered in equation 2.12 (Hu & Tao, 2016). Equation 2.13 below used to calculate the charges, where  $D$  is the integration on electrode areas and  $\sigma$  is stress field.

$$D = d\sigma \quad (2.13)$$

PVDF can also be utilized as a pyroelectric material since it can display  $P_s$  when no electric field is applied. Temperature fluctuations ( $dT/dt$ ) generate electricity in pyroelectric materials, which is analogous to piezoelectric harvesters, which convert mechanical oscillations ( $d\sigma/dt$ ) to electric energy.

The generated pyroelectric current ( $I_p$ ) is defined using Equation 2.14 when the temperature ( $dT/dt$ ) changes:

$$I_p = \frac{dQ_T}{dt} = \rho A \frac{dT}{dt} \quad (2.14)$$

Where  $Q_T$  denotes the pyroelectric charges,  $A$  denotes the material's surface area, and is the pyroelectric coefficient.

(Tao & Hu, 2016) stated in their study that PVDF films will affect the pyroelectric coefficients. When the film is completely clamped and under constant strain with uniform heat distributions, the main pyroelectric effect is best achieved. When the film is not clamped and is allowed to deform with temperature changes, the secondary pyroelectric effect occurs, affecting the thermal expansion/contraction strain and modulating the polarization via the piezoelectric effect. The particular temperature gradient of the film, which produces the tertiary pyroelectric effect, causes shear stress, which can change polarization.

Pyroelectric materials have been used in a wide range of PyEH applications, including heat sensors, thermal imaging or infrared sensors, fire alarms, and gas sensors, in both bulk and thin-film forms. Several ferroelectric materials, including PMN-PT and PLZT, as well as polymers like PVDF-TrFE, have been studied for wearable and plantable devices on the human body. Polymers are desired for their inexpensive cost, light weight, flexibility, and biocompatibility. PVDF is also the best material for fabricating flexible hybrid energy cells because it has both piezoelectric and pyroelectric capabilities, superior mechanical characteristics, geometrical effect, and great sensitivity to minor mechanical stress and deformation.

## **2.9 Hybrid Piezo-pyroelectric system**

By combining two or more energy sources in one device, hybrid systems were introduced. Energy sources like pyroelectric energy, piezoelectric energy, thermoelectric energy and photothermal energy will be combined thus create hybrid energy harvester. As a result, by utilizing more energy sources, efficiency can be improved. All piezoelectric materials are pyroelectric because the pyroelectric effect is caused by spontaneous polarization inside the material when subjected to temperature changes. Table 2.2 compares related equations for pyroelectrics subjected to temperature change ( $\Delta T$ ) and piezoelectric subjected to stress ( $\Delta\sigma$ ) and their similar in both open and closed circuits, relationships between current, voltage, and stored energy are studied in relation to temperature change and applied stress.

**Table 2.2 : Equations for pyroelectrics and piezoelectric (Bowen et al., 2018)**

	Pyroelectric	Piezoelectric
Charge ( $Q$ )	$Q = p A \Delta T$	$Q = d_{ij} A \Delta \sigma$
Short-circuit current ( $i = p A \Delta T / \Delta t$ )	$i = p A \frac{\Delta T}{\Delta t}$	$i = d_{ij} A \frac{\Delta \sigma}{\Delta t}$
Open-circuit voltage ( $V = Q/C$ )	$V = \frac{p}{\epsilon_{33}^T} h \Delta T$	$V = \frac{d_{ij}}{\epsilon_{33}^T} h \Delta \sigma$
Stored energy ( $\frac{1}{2}CV^2$ )	$E = \frac{1}{2} \frac{p^2}{\epsilon_{33}^T} A h (\Delta T)^2$	$E = \frac{1}{2} \frac{d_{ij}^2}{\epsilon_{33}^T} A h (\Delta \sigma)^2$

Due to a combination of temperature change and applied stress, a prospective hybrid piezo-pyroelectric harvesting system has piqued interest. Because the frequency and vibration for each system are different, (Bowen et al., 2018) states that it is necessary to tune the electronics for hybrid systems. (Bowen et al., 2018) research. Using a micro-patterned piezoelectric PVDF- TrFE polymer, a micro-patterned PDMS-CNTs composite, and graphene nanosheets, researchers developed a stretchable, hybrid piezo-pyroelectric nano-generator. Along with its high thermal conductivity, graphene was used as a top flexible electrode to allow for a quick temperature gradient. PDMS-CNTs was used to make the device flexible and to serve as a strong electrode on the device's base. The total polarization shift is depicted below:

$$\Delta P = d\sigma + p\Delta T \quad (2.15)$$

Where  $\Delta P$  represents polarization change,  $d$  represents piezoelectric coefficient,  $\sigma$  represents stress, and  $p$  represents pyroelectric coefficient.

Sometimes, beam vibration and thermal cycling combination gives negative impact on scavenged energy, revealing potential contact complications, such as temperature and mechanical oscillation frequency differences.

## 2.10 Summary of previous research device

Piezoelectric energy had been discovered a long time ago. Therefore, a lot of researchers had done investigation on it so that it can be harvested to form a useful energy. Table 2.3 shows the summarization of previous research that had been done on certain piezoelectric material and its configuration used to harvest the energy.

**Table 2.3: Summary of previous research on piezoelectric material and configuration**

Title	Material	Configuration	Size piezoelectric material	Power Output
Thermal Energy Harvesting Using Pyroelectric and Piezoelectric Effect	PZT-5H	Using bimetal beam, composed of Fe-Ni and Fe-Ni-Cr	50mm x 0.9mm x 0.127mm	0.54 $\mu$ W
Hybrid Energy Harvester Using Piezoelectric and Pyroelectric Properties of PZT-5A Ceramics	PZT-5A	Using aluminium cantilever by using silver epoxy	5mm x 10mm x 0.5mm	Voltage in mV

Performance of Thin Piezoelectric Materials for Pyroelectric Energy Harvesting	PZT-5A, PMN-PT, PVDF	Thin sample element was bonded to thin resistance	PZT-5A (150 $\mu$ m), PMN-PT(273 $\mu$ m), PVDF (110 $\mu$ m)	PZT-5A (0.33 $\mu$ W), PMN-PT (0.35 $\mu$ W), PVDF (0.26 $\mu$ W)
Energy harvesting from pavement via polyvinylidene fluoride: hybrid piezo-pyroelectric effects	PVDF	Using aluminium beam, an electrical insulation layer was added between the material sample and the beam and electrodes was mounted on the PVDF sample.	25.4 mm x 25.4mm	Voltage in mV
Modelling of an Energy Harvesting Piezoelectric Cantilever Beam	PZT	Using unimorph cantilever beam (two-layered bending element)	1mm	0.9mW

Design and Simulation of Piezoelectric Cantilever Beam Based on Mechanical Vibration for Energy Harvesting Application	PZT-5H	Cantilever Beam using copper as substrate	12mm x 2.5mm x 0.03mm	595.5mV
Design and Simulation of a Piezoelectric Cantilever Beam for Mechanical Vibration Energy Harvesting	PZT-5A	Bimorph cantilever beam using copper as elastic layer	10mm x 10mm x 0.1mm	2mW

## CHAPTER 3

### METHODOLOGY

#### 3.1 Methodology

This chapter will discuss about the design and simulation of piezo-pyroelectric energy harvesting device. This piezo-pyroelectric energy harvesting device is used to power up air-conditioner temperature sensor with rated power of 20mW. This research proposing piezo-pyroelectric energy harvesting device which consists of piezoelectric material with thickness of 5mm deposited with flexible substrate using HDPE (high-density polyethylene). These substrates to maintain its flexibility. The piezoelectric material using 100mm X 80mm dimension. Piezoelectric material used for this project is PVDF (polyvinylidene fluoride) with 200mm X 80mm and copper (Cu) for electrode. In this chapter, the design and simulation on the performance of the energy harvesting device were discussed. Theoretical calculations were implemented to prove the power output of the device.

#### 3.2 Flowchart

Flowchart in figure 3.1 shows the step of procedure to run this study. Draft of device design is the first before starting the simulation. After that, theoretical calculation is performed to the suitable dimension for the device. After obtaining the suitable power harvest from the device, the design will be completed. Before starting the simulation, all parameter that will be used during the simulation will be set. After setting all the parameter, the simulation can be performed, and the result obtain will be checked to ensure the result produce is acceptable. If the results obtained is not acceptable, thus the parameter need to be changed and new simulation will be performed until good result is obtained.

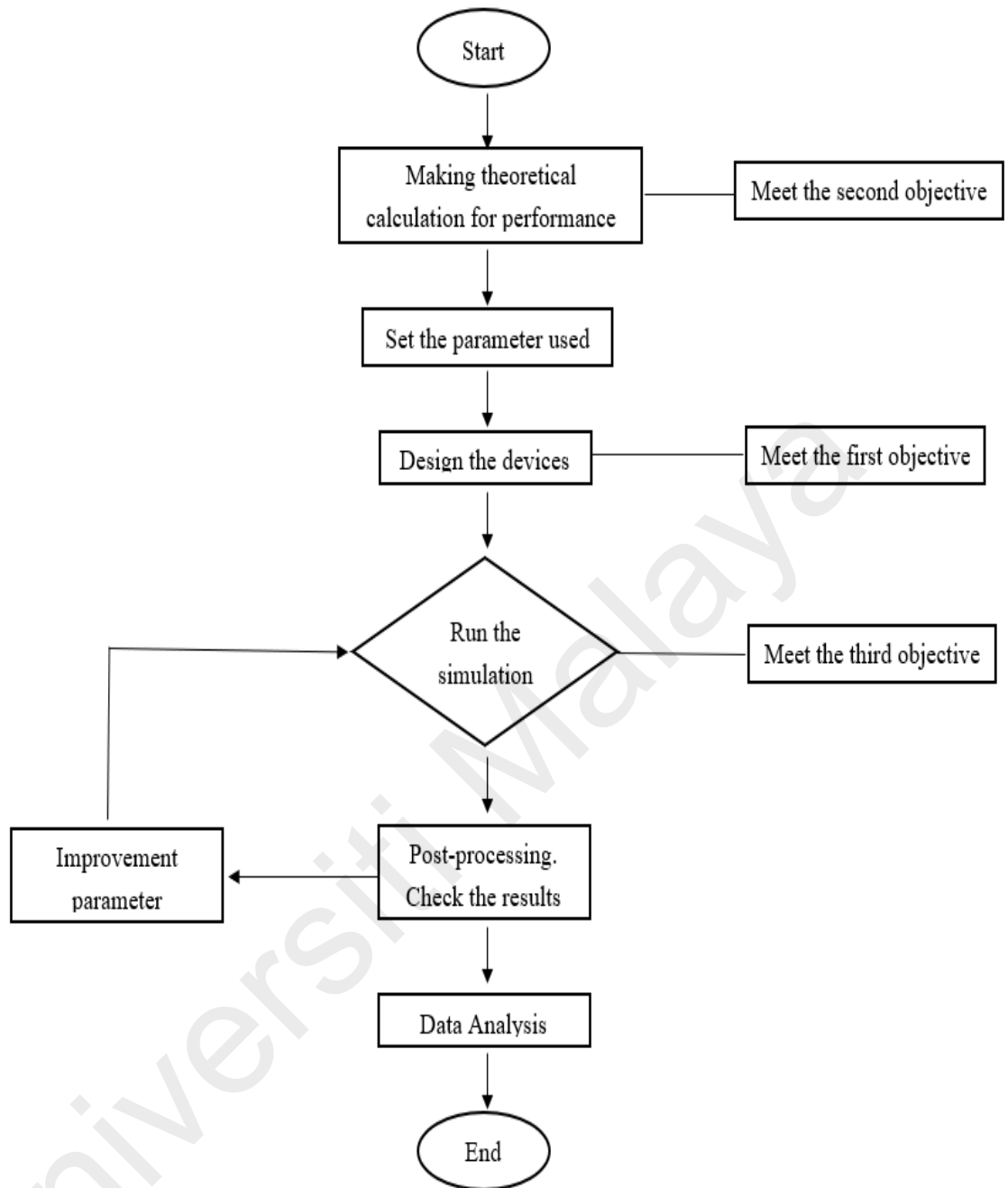


**Figure 3.1: Flowchart of the project**

### 3.3 Selection of material

The selection of the material had been a crucial part in this project since it need to harvest both piezoelectric and pyroelectric energy. In this project, piezoelectric material used is polyvinylidene fluoride (PVDF) as it can possesses both piezoelectric and pyroelectric energy, as demonstrated in Chapter 2 by its exceptional flexibility, chemical

resistance, thermal stability, and mechanical properties. When mechanical stress or deformation is applied to PVDF, the direction of the electric dipoles changes, resulting in an accumulation of charges on the electrode surfaces. It also can be used as pyroelectric material since when there is no applied electric field, it can exhibit a spontaneous polarization ( $P_s$ ). Results from experiment done by (Hu & Tao, 2016) demonstrates that the piezo-pyroelectric hybrid effect is equal to the algebraic sum of the individual piezoelectric and pyroelectric effects, and that there is no coupling effect when PVDF is used. This shows during piezoelectric energy harvesting process, pyroelectric cannot be neglected when using PVDF material. From (Zi et al., 2015) experiment, it can deliver a high short-circuit current from the piezoelectric effect and a high open-circuit voltage from the pyroelectric effect, according to the results (Zi et al., 2015). Although PVDF shows the lowest performance on pyroelectric energy harvesting compared to PMN-PT and PZT-5A based on (Xie et al., 2010) research, but it still suitable for this project since this project only focusing low grade heat applications. (Thakre et al., 2019) stated PVDF is suitable for large-area thin films because of its ease of production, stability when exposed to heat, vacuum, moisture, and mechanical resilience, according to the researchers. PVDF also preferred due to its low heat conductivity, low permittivity, and its low dielectric constant. Furthermore, its high sensitivity for small mechanical stress and deformation, improved mechanical properties and geometrical has attracted much interest to use this material for energy harvesting. Table 2 below shows the comparison generated peak power for piezoelectric materials stated in (Covaci & Gontean, 2020) research.

**Table 3.1 : Generated peak power for piezoelectric materials**

Piezoelectric Material	Peak Power (mW)	Volume	Frequency (Hz)
PVDF [87]	0.61	$72 \times 16 \times 0.41$ mm	2
PZT ceramic [88]	52	$1.5$ cm <sup>3</sup>	100
PZT fiber [89]	120	$2.2$ cm <sup>3</sup>	-
PMN-PZT single crystal [90]	0.015	$20 \times 5 \times 0.5$ mm	1744
PMN-PT single crystal [91]	3.7	$25 \times 5 \times 1$ mm	102

### 3.4 CAD Design

CAD or known as Computer Aided Design is a computer software used to design and document a product. CAD also be define as subset of design process (Zeid, 2004). It enables engineers to develop, modify and optimized the design process (Academy, 2021). Three discipline is utilize in CAD design which is geometric modeling, computer graphics and design (Academy, 2021).

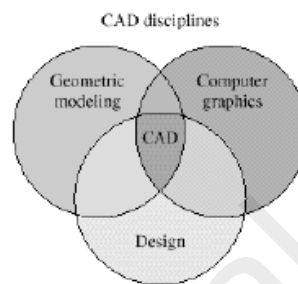


**Figure 3.2 : Discipline in CAD design (Zeid, 2004)**

CAD processes includes drafting, dimensioning, assembly modelling, documentation, and tolerancing. CAD helps creating designs in 2D and 3D form so that designer can visualize the design. Preliminary design and layouts, design details and calculations, construct 3D models, creating and releasing drawings and interfacing with analysis, marketing, manufacturing and as well as end-user personnel can be performed by CAD (Academy, 2021). Any object design in 2D can be viewed from any angle, including top, bottom, and side views, whereas 3D views are similar to 2D and addition can be viewed in isometric view.

2D CAD rely on usage of basic geometric shapes like lines, circles, rectangles, triangles, points and etc to produce flat drawings (Academy, 2021). On the other hand, 3D is a popular design tool as it allows the creation of 3D images which makes it more realistic and imaginable. The model can be viewed and rotated in X, Y and Z axis. These 3D images view is called isometric view. 3D CAD is the repretation of intensify from 2D CAD software. In this study, SolidWorks is used to design the hybrid piezo-pyroelectric conversion device

### **3.5 Multiphysics Modeling Method**

Multiple coupled physics impact on designs simultaneously in real-world product contexts (ANSYS, 2010). In multiphysics modeling, heat is generated by the flow of electric current, mechanical stresses are created by fluid pressures, and thermal stresses are produced by temperature gradients. Engineers and designers can minimize error margins, improve product reliability, and build more inventive product designs by introducing multiphysics simulation into the design process. This study using ANSYS as the simulation software for analytical calculation. ANSYS multiphysics simulation is a combination of high-fidelity engineering analysis tools that allow engineers to forecast real-world behaviour precisely (ANSYS, 2010).

#### **3.5.1 Direct Coupled-field Elements**

By occupy a single finite element model with relevant coupled-physics options set within the element itself, a coupled-physics problem can be solved (ANSYS, 2010). The modeling of multiphysics problem can be simplify by allowing users to build, solve, and post-process a single analysis model for a wide variety of coupled-field problems using a direct coupled-field solution. These type of solutions generally use for thermoelasticity, piezoelectricity, piezoresistivity, the piezocaloric effect, the Coriolis effect, electroelasticity, thermoelectricity and thermal-electric-structural coupling application (ANSYS, 2010). Since this study harvesting energy from piezoelectric material thus these type of simulation has been used to collect range of data and graph from the energy harvest.

### **3.6 Design Consideration**

Piezo-pyroelectric energy in this project is harvest from condenser of air conditioner. Piezoelectric energy is harvest from the vibration produced from the hot air flow produce from the condenser fan while pyroelectric energy is harvest from the temperature of hot air flow. In this study 20mW is the target power output to achieve to power up the

temperature sensor in condenser. Study by (Koyuncuoglu et al., 2013) using unimorph cantilever with cantilever size of 70mm x 10mm x 2mm and PZT size of 5mm x 10mm x 0.5mm. The maximum voltage produce at 6 Hz frequency is around 379 mV. According to study by (Kang & Yeatman, 2016) using unimorph configuration, indicate that maximum power output produce is 0.54 $\mu$ W with load resistance of 610 k $\Omega$ , velocity of 12mm/s at 0.05 Hz. The bimetal beam used in the study is 50mm x 0.9mm x 0.5mm while PZT used is 50mm x 0.9mm x 0.127mm. Other than that, studied by (Kundu & Nemade, 2016) mentioned they modeling a composite cantilever which consists three layers with the same thickness and a mass attached at the end of the beam symmetrically. In the study mentioned that harvested power around 0.323mW with same model dimension of beam, piezoelectric layer (PZT-5H) and substrate layer of 50mm x 5mm x 0.5mm. The end mass dimension used in this study is 10mm x 5mm x 7.8mm. Whereas study by (Hu & Tao, 2016) indicate that by using PVDF film of 25.4mm x 25.4mm, the voltage produce from the energy harvesting is in mV. This shows that PVDF produce lower power than PZT material. Thus bigger dimension needed to harvest 20mW to power up temperature sensor. As shown in subchapter 2.4, there are two type of mode generator which is  $d_{31}$  (longitudinal mode) and  $d_{33}$ (transerve mode). In this project,  $d_{33}$  mode are consider as the cantilever beam stress/strain produced along the horizontal direction as the electric field applied in vertical direction (Covaci & Gontean, 2020). The compressor used for this project as medium is Goodman Air Conditioner Condenser with Heat Pump. Figure 3.1 shows the air conditioner illustration and its dimensions and table 3.2 shows the specifications of the air conditioner :

**Table 3.2 : Specifications of Goodman Air Conditioner Condenser with Heat**

**Pump:**

Specification	Value
Nominal capacity (tons)	1.5
Nominal capacity (Btu/h)	18000
Heating capacity – Heat pump (Btu/h)	18000
Heating method	Heat pump
Operation mode - HVAC	Cooling / Heating
Amps	11.8 A
Voltage	208 / 230V AC
Phase	1
Hz	60
SEER	14
Liquid line size	3/8 in
Suction line size	3/4 in
Refrigerant type	R-410A
Height	34 ¼ in
Width	29 in
Depth	29 in

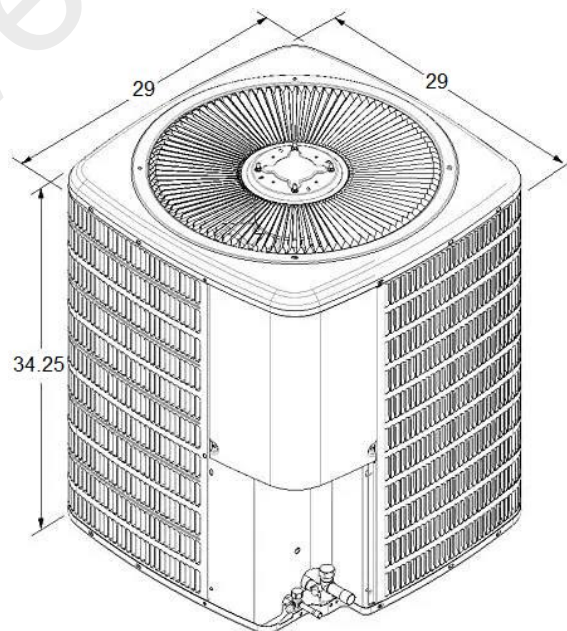


**Figure 3.3 : Dimension for air-conditioner condenser**

### 3.6.1 Theoretical calculation

Since the power needed to be generated is 20mW. Thus dimension shown in table 3.3 is used to design the device after analyzing previous study and carrying out calculations with various dimensions. Theoretical power needs to be calculated to compare the result with analytical calculations. These are crucial since we need to know how much device will be needed to power up the temperature sensor from energy harvesting. Table 3.4 below shows the parameters for PVDF material used in this design. The parameters were used to calculate the power output produced by the piezo-pyroelectric device.

The parameters used to design the device and parameters for theoretical calculation are present in table 3.3 & table 3.4 as below :

**Table 3.3 : Parameter of the design**

Parameter	Value
Beam configuration	Bimorph
Length of PVDF sheet	100mm
Width of PVDF sheet	50mm
Thickness of PVDF sheet	1mm
Length of copper electrode	70mm
Width of copper electrode	50mm
Thickness of copper electrode	0.5mm
Length of HDPE layer	200mm
Width of HDPE layer	50mm
Thickness of HDPE layer	3mm

**Table 3.4 : Parameter used for theoretical calculation**

Parameter	Value
$d_{33}$ (piezoelectric strain constant)	33 pC/N
$g_{33}$ (piezoelectric stress constant)	330e-3 m <sup>2</sup> /C
$\epsilon_0$ (relative permittivity)	8.85 pF/m
$\epsilon_r$ (relative dielectric constant)	12
$p$ (pyroelectric coefficient)	30 $\mu$ C/m <sup>2</sup> .K

Therefore when force being applied to the device, it will produce vibration and thus the electrostatic equation of piezoelectric effect can be derived as :

$$Q_{33} = d_{33}F_{33} \quad (3.1)$$

$$V_{33} = \frac{T}{WL}F_{33}g_{33} \quad (3.2)$$

Where T is the thickness of the PVDF used, W is the width of the PVDF material, L is the length of the PVDF and F is the force exerted on the PVDF material.  $d_{33}$  is the piezoelectric strain constant of PVDF for mode  $d_{33}$  and  $g_{33}$  is the piezoelectric stress constant of PVDF in  $d_{33}$  mode. Furthermore, when there is thermal change, it produces pyroelectric effect and the charge can be calculated as equation :

$$Q = pA\Delta T \quad (3.3)$$

Where p is pyroelectric coefficient of PVDF and A is the area of PVDF used to harvest the energy. Then, the total of charge produced from piezoelectric and pyroelectric effect can be derived as :

$$Q_T = Q_{piezo} + Q_{pyro} \quad (3.4)$$

Then, from the charge produced, current can be calculated by using the formula :

$$I = \frac{Q_{Total}}{t} \quad (3.5)$$

Where Q is total charge produced and t is the time period of the produce current. By assuming the charge produced in one minute, the current produce from the device is calculated. Then, the power output produced from piezoelectric energy can be calculated as :

$$P = IV \quad (3.6)$$

Table 3.5 and 3.6 shows the power and voltage output produce from the range of force and heat temperature applied for theoretical calculation.

**Table 3.5: Theoretical calculation for heat temperature difference**

F (N)	$\Delta T$ (K)	$Q_{pyro}$ (C)	$Q_{piezo}$ (C)	Current, I (A)	Voltage (V)	Power (W)
5	14	2.1E-06	3.3E-11	0.0021	0.660	2.772E-03
5	16	2.4E-06	3.3E-11	0.0024	0.660	3.168E-03
5	18	2.7E-06	3.3E-11	0.0027	0.660	3.564E-03
5	20	3.0E-06	3.3E-11	0.0030	0.660	3.960E-03
5	22	3.3E-06	3.3E-11	0.0033	0.660	4.356E-03

**Table 3.6: Theoretical calculation for force difference**

F (N)	$\Delta T$ (K)	$Q_{pyro}$ (C)	$Q_{piezo}$ (C)	Current, I (A)	Voltage (V)	Power (W)
1	14	0.0000021	3.3E-11	0.0021	0.132	0.554E-03
2	14	0.0000021	6.6E-11	0.0021	0.264	1.109E-03
3	14	0.0000021	9.9E-11	0.0021	0.396	1.663E-03
4	14	0.0000021	1.32E-10	0.00223	0.528	2.218E-03
5	14	0.0000021	1.65E-10	0.00227	0.660	2.772E-03

Thus, the highest power output produced from the device based on heat temperature difference is 4.36 mW while for force difference is 2.77mW. As conclusion, 5 devices are needed based on highest power output produce from temperature difference to gain sufficient power to power up the sensor based on theoretical calculation. Whereas 8 devices are needed to power up 20mW based on highest power output produce from force difference.

### 3.7 Design of hybrid piezo-pyroelectric device

In this design, bimorph cantilever beam piezoelectric configuration is applied to harvest piezoelectric and pyroelectric energy. As discussed, bimorph configuration said as most suitable configuration for low frequency and resistance. From (Poh et al., 2018) research, they indicate in terms of energy harvesting, bonded bimorph beam configuration more effective as energy output produce from the harvesterdoubles. Output voltage can

boost since two piezoelectric parts were used in bimorph configuration by opposite strain during the operation. Additionally, electromechanical coupling capability of a piezoelectric bimorph cantilever beam improved as observed by (Poh et al., 2018). (Kundu & Nemade, 2016) mentioned that electrodes formed from metalizing the top and bottom surfaces of bimorph configuration can be wired as parallel and series connection. Figure 3.4 shows the illustration.

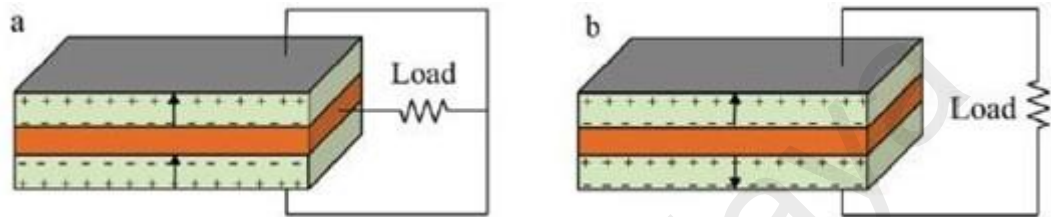


**Figure 3.4 : Illustration of parallel (a) and series (b) connection in bimorph (Kundu & Nemade, 2016)**

In his study also indicate that metallic electrodes charge can be generate due to moment form from motion of the end mass exerts stress on the piezoelectric material. The piezoelectric layer experience strain along x-direction as input vibration assume to be in z-direction. He illustrated the diagram as in figure 3.5.

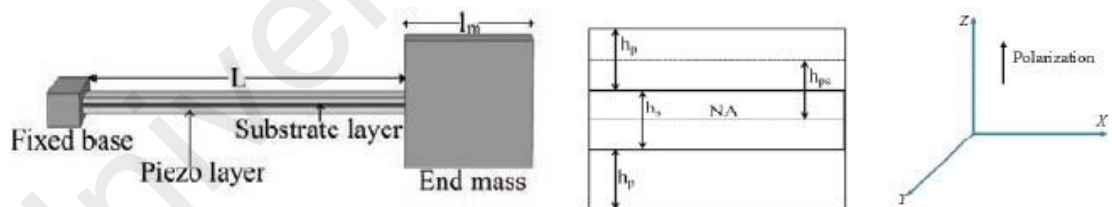


**Figure 3.5: Schematic diagram of energy harvester and cross-sectional view of bimorph**

where NA indicate the neutral axis of beam,  $h_p$  and  $h_s$  are piezoelectric and substrate layer thickness while  $h_{ps}$  represent distance between center of piezoelectric layer and the neutral axis of the beam (Kundu & Nemade, 2016).

### 3.7.1 Device design

The device is designed using SolidWorks software where all parameter design used is indicate in table 3.3. Some parameters in this study need to be maintained constant to obtain an accurate comparative analysis such as the dimension of electrode layer, piezoelectric layer and cantilever beam. Figure 3.6 shows the isometric view hybrid piezo-pyroelectric device design. The figure shows the position of the device above the air condenser. Basically, the bimorph cantilever beam piezoelectric configuration was placed on top of two plate. The plate was mounted on top of hollow structure. Figure 3.7 shows the details of the device structure mounting.

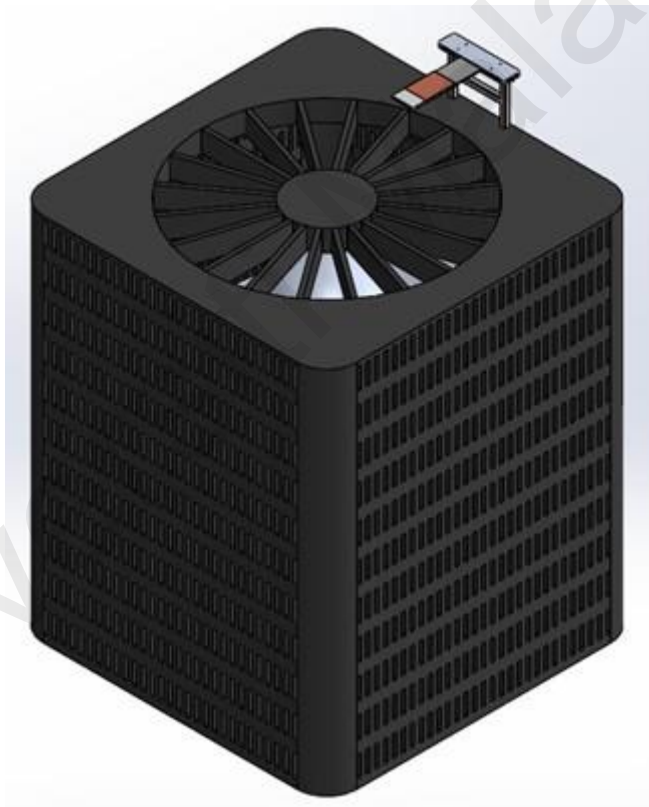


**Figure 3.6: Isometric view for the device position**

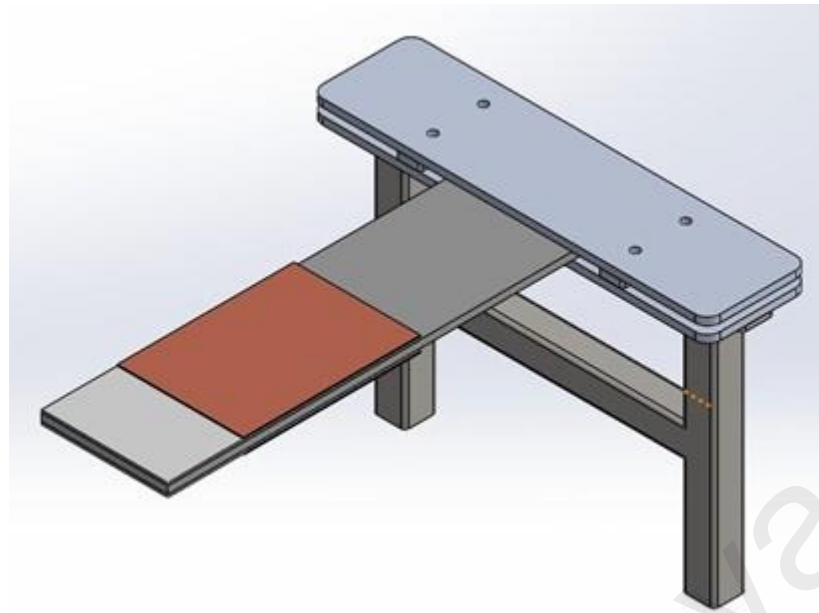


**Figure 3.7: Isometric view details of the device mounting structure**

The piezoelectric layer modelled as PVDF dimension has been set to 100 x 50 x 1 (length x width x thickness) in mm. Additionally, the cantilever beam design as HDPE sandwiched between two piezoelectric layers. Its dimensions are 200 x 50 x 3 (length x width x thickness) in mm. Next, charge conductor sandwiched between two layers of piezoelectric layers which is copper with dimension 70 x 50 x 0.5 (length x width x thickness) in mm. The figure 3.8 shows the layering details for the device. The first layer and fifth layer represent the copper electrode while the second and fourth layer represent the piezoelectric material which is PVDF. Lastly, the center layer or the third layer is HDPE. Figure 3.9 shows the isometric view of cantilever configuration. Dimension of the cantilever design is shown in figure 3.10.

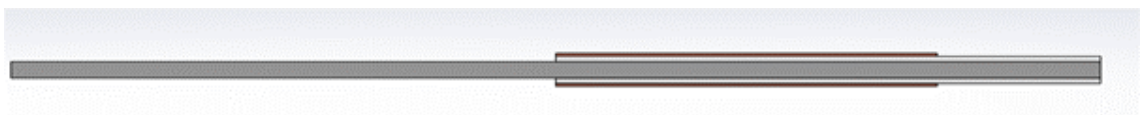


**Figure 3.8: Details of cantilever configuration**

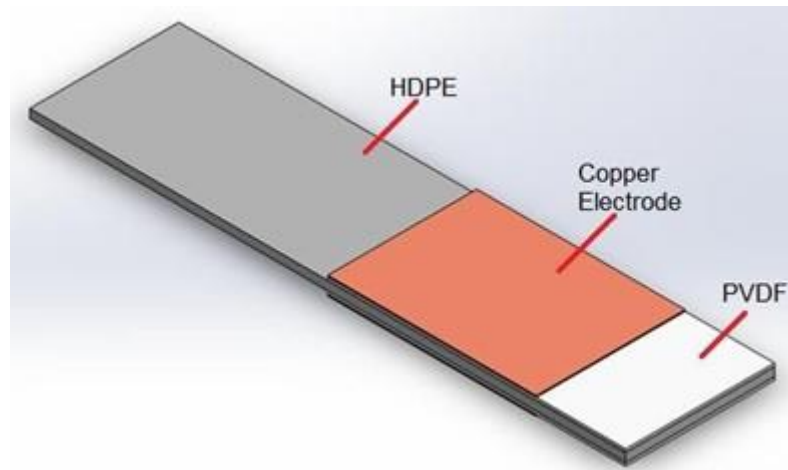


**Figure 3.9: Isometric view of cantilever configuration**

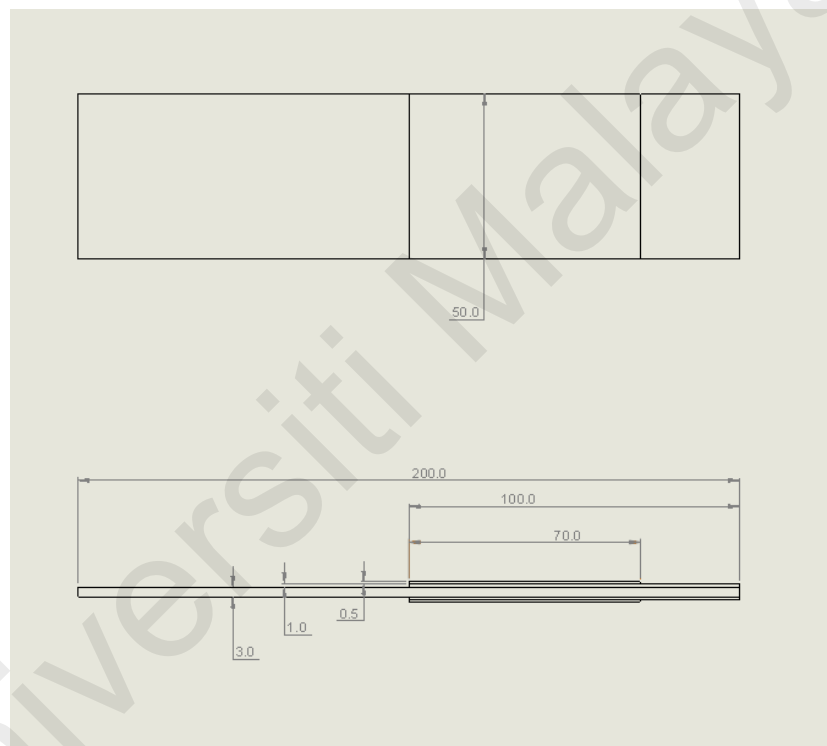


**Figure 3.10: Cantilever design dimension**

In this study, HDPE was chosen due its elasticity, higher working heat temperature, higher tensile strength and better resistance to heat. Since, this study involving heat temperature changes to harvest energy, hence high melting point must be considered. Moreover, it is relatively stronger, and any excess of vibration must be avoided. Subsequently, HDPE is a good electrical insulation. Accordingly, this is a good advantageous for this study since the energy harvest can be flowed to other layers. Next,

in this study the usage of electrode is a demand as the electrical current need to be transferred. As it is commonly used as a base metal for electrical contact and electrode applications. Copper was selected as electrode in this study due to its electrical conductivity. Roughly copper is commonly used as an electrode due its high thermal and electrical conductivity. These properties are needed in this study since there is thermal involved during energy harvest. Besides, these energies need to be transferred to other layer in electrical form.

### **3.8 Simulation**

Simulation in this study is done using ANSYS software. The simulation using piezoelectric and MEMS extension by ANSYS. These extension function to help integrate area piezoelectric & MEMS application in mechanical. According to (Dudhat et al., 2019) in his study, the extension consists of one XML file which configures the UI content and one pythom script to implement the extension functionality.

Since piezoelectric & MEMS is applied, thus all the equation and calculation done are based on piezoelectric application. Hence, no APDL command required in this simulation. Before starting the simulation, the engineering data, mesh and setup need to be set first. In this study, the analysis used to generate power is Modal analysis, Harmonic Response and Static Structural. Flowchart in figure 3.11 shows the step of simulation analysis for this study to obtain specific result to get the power generated by the device.

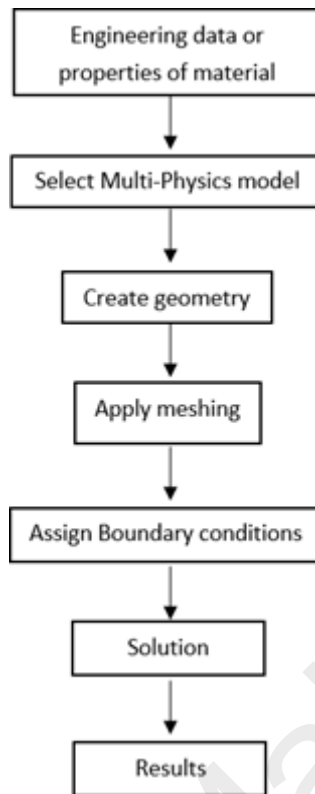


**Figure 3.11: Flowchart of simulation**

### 3.8.1 Engineering data

In table 3.7 shows the material properties of copper, PVDF and HDPE set in engineering data properties.

**Table 3.7: Material properties for copper, PVDF and HDPE**

	Copper	PVDF	HDPE
Density (kg/m <sup>3</sup> )	8960	1880	970
Specific heat capacity (J/kg. K)	383	1500	1900
Young's Modulus, GPa	124	2	1.2
Tensile Strength, MPa	220	43.4	23
Thermal conductivity, W/m. K	386	0.19	0.52
Poisson's ratio	0.34	0.3	0.46
Coefficient of thermal expansion (x10 <sup>-6</sup> ) (K <sup>-1</sup> )	17	128	100

### 3.8.2 Geometry

In geometry stage, the bimorph layering configuration design using SolidWorks being export into geometry. The model is design based on the parameter set in table 3.3. Figure 3.12 shows the illustration of the geometry produce after it is being export.

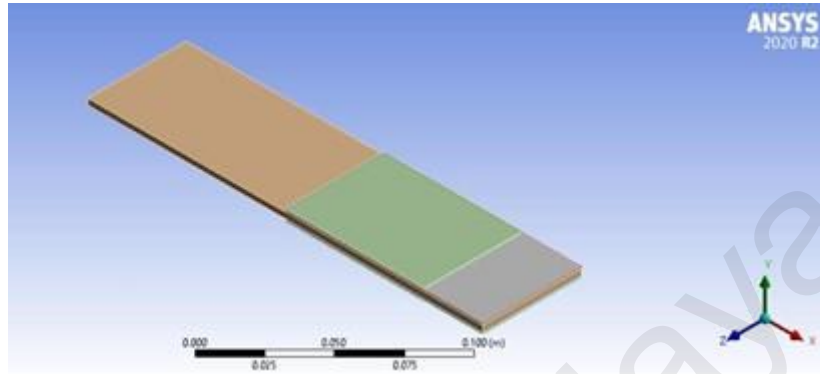


**Figure 3.12: Geometry of hybrid piezo pyroelectric**

### 3.8.3 Modeling

Modeling stage involving meshing process. The mesh is done to get better result. As finer the mesh, more accurate the result. The same mesh is applied to all simulation. The meshing is done by applying element size and body sizing element size mesh. The mesh is applied on all bodies and body sizing is applied on body involved with heating. Figure shows the meshing produce on all bodies after mesh is applied. Table 3.8 below shows the no of elements and no of nodes produce for piezoelectric mesh.

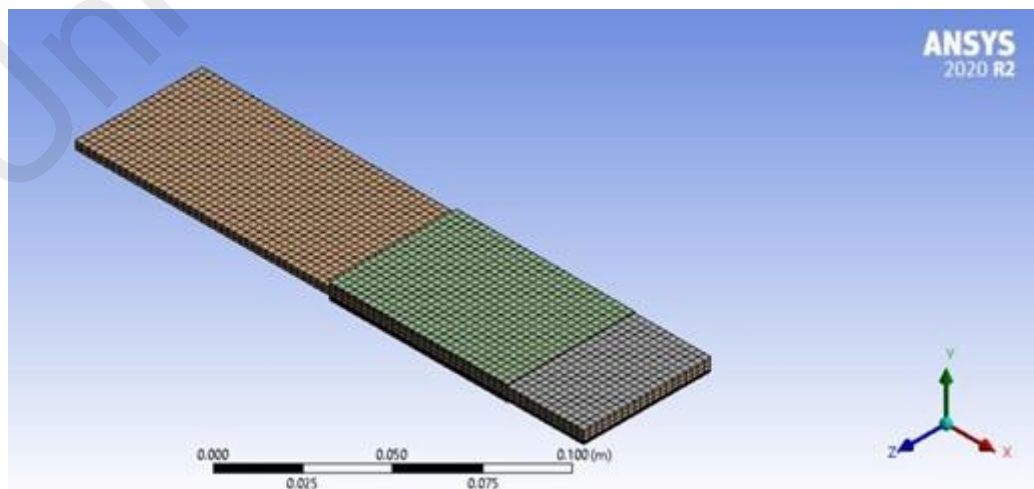


**Figure 3.13: Meshing for piezoelectric**

**Table 3.8: No of elements and nodes**

Element size (mm)	Body sizing (mm)	No of nodes	No of elements
3.0	2.0	37884	10636

### 3.8.4 Setup

After mesh is applied, so next step in ANSYS simulation is setup. In this stage, parameter is set to harvest hybrid piezo-pyroelectric energy. To calculate the result, certain parameter needs to be applied first in the simulation in order to harvest piezo-pyroelectric energy. Figure 3.13 shows the fixed support for the application. For the force assumption, 5N is applied because we need higher force to create higher stress. Based on previous study, most of the study applied huge load resistance so that higher power output produces from energy harvesting. Thus, this number is selected since it is suitable for the application for condenser since condenser release quite powerful wind. For the PVDF heat temperature, top PVDF heat temperature is assume based on this country environment temperature during sunny day and for bottom 5 value of parameter was chosen because usually the air heat release by condenser is around 40°C to 60°C.

**Table 3.9: Parameter used in setup**

Parameter	Value
Force	5N
Heat temperature top PVDF	36°C
Heat temperature bottom PVDF	50°C
Acceleration	1m/s <sup>2</sup>

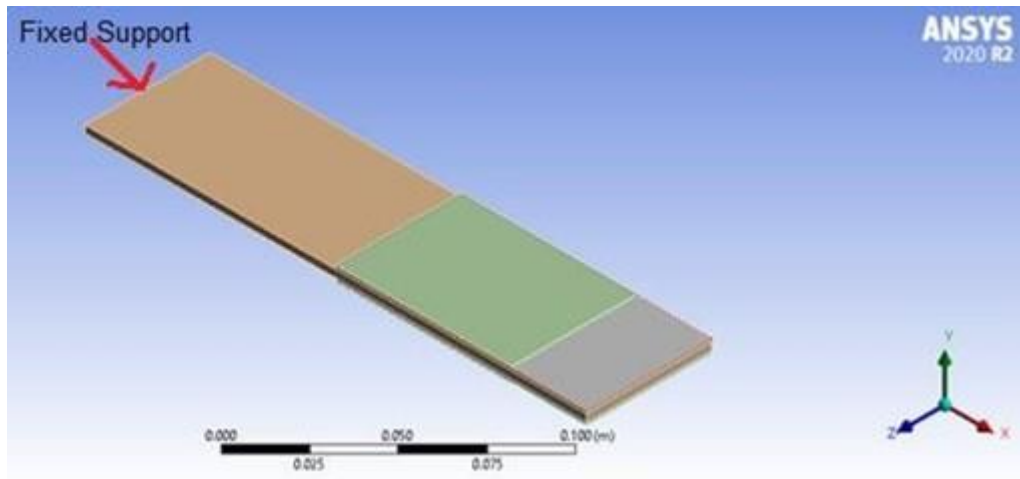


**Figure 3.14: Fixed support of the device**

### 3.8.5 Analysis

Four different analyses involved in this study to get the performance result for the device:

- 1) Static structural
- 2) Modal
- 3) Harmonic Response

Based on (Dudhat et al., 2019), modal analysis is used to perform natural frequencies of combined system. In this study, it involved cantilever beam (HDPE) and piezoelectric material (PVDF). A fixed support is applied at the end of the structure as in figure 3.14. Top PVDF material is set into piezoelectric body and bottom is set as thermal-piezoelectric body. Thermal condition is applied to top PVDF and bottom PVDF. Force is applied at the bottom PVDF. Static structural helps to get the voltage output for the piezoelectric material (Dudhat et al., 2019). Furthermore, harmonic response is applied to turn induce strain in the piezoelectric layer to generate voltage. Figure 3.15 shows the sequence for the simulation of analysis hybrid piezo-pyroelectric device.

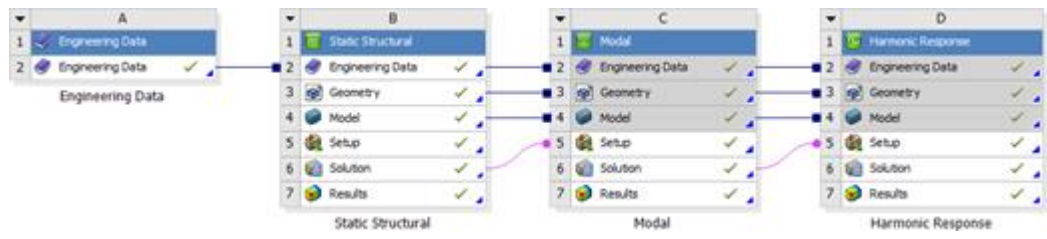


**Figure 3.15: Analysis system of hybrid simulation**

Universiti Malaya

## CHAPTER 4

### RESULTS & DISCUSSION

#### 4.1 Introduction

In this chapter will show the result from the simulation run and discussion on the comparison of theoretical results and analytical results. 5 range of data is used to plot every graph in this study. Figure 4.1 until 4.4 shows the deformation of one of the simulations produce. It shows the deformation of the device during the simulation when all different parameter of force and heat temperature is applied. The red color indicates the maximum value of deformation while dark blue shows the minimum value of deformation. From the figures shows that each maximum deformation produce for every frequency is different. Since the fixed support on the left side of the device thus the minimum value is always on the same side of the device. In figure 4.4 shows that the maximum deformation generate during frequency 2490.5 Hz is very high among other frequency which 15.817.

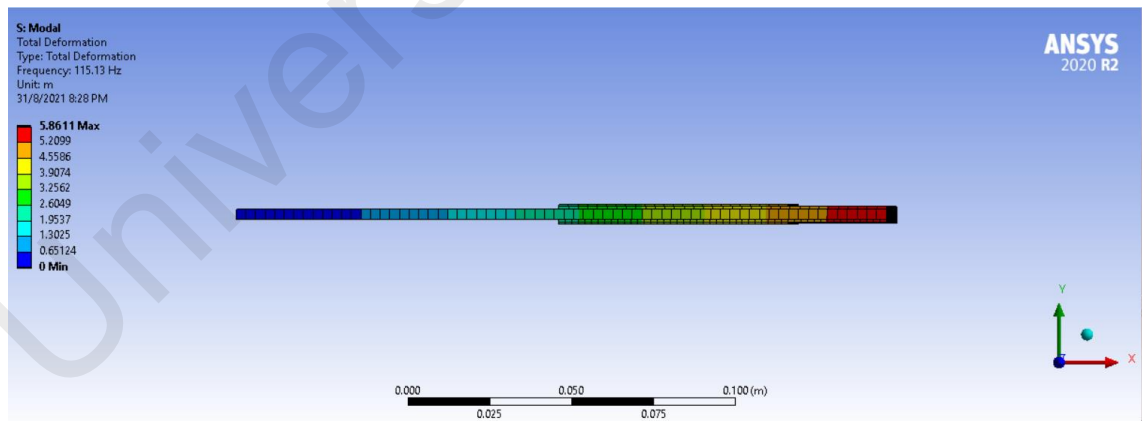
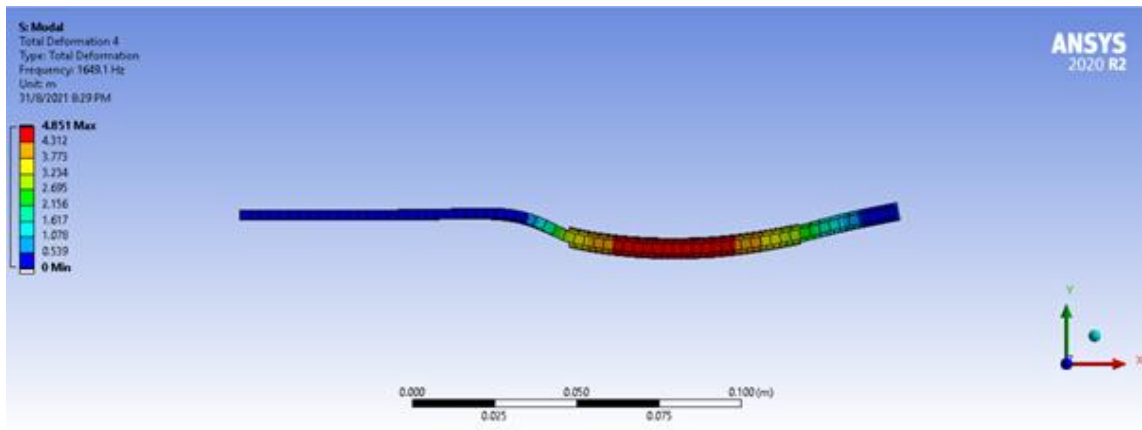
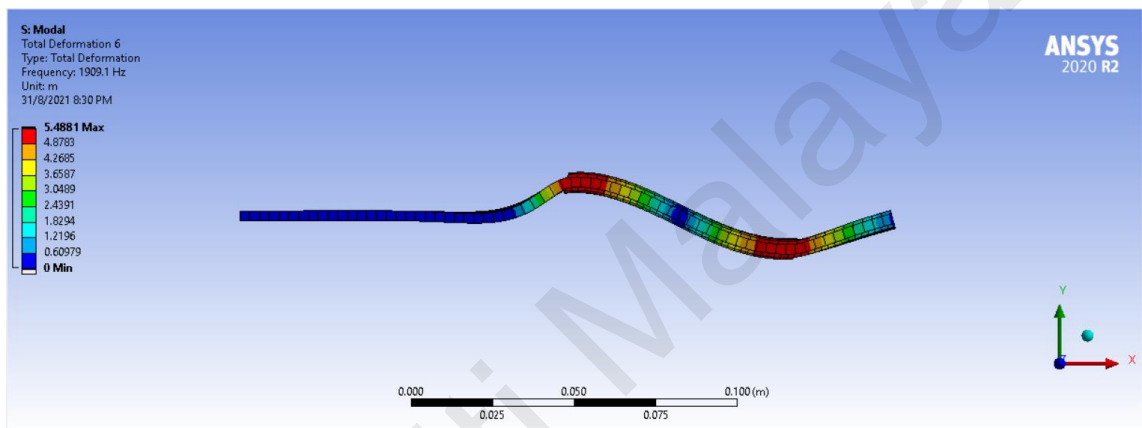


Figure 4.1: Deformation during frequency 115.13 Hz



**Figure 4.2: Deformation during frequency 1649.1 Hz**



**Figure 4.3: Deformation during frequency 1909.1 Hz**

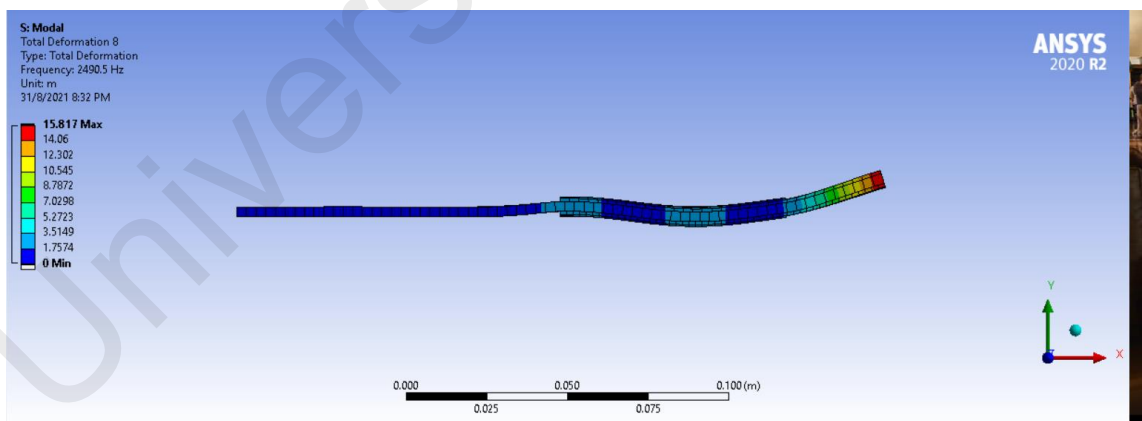


**Figure 4.4: Deformation during frequency 2490.5 Hz**

## 4.2 Results

This section showing the results of power output from theoretical and analytical calculation and their comparison in a graph for every different parameter used. The voltage output and displacement results also shown in this section.

#### 4.2.1 Effect of heat temperature difference on power performance

In this section, the result for simulation involves 5 different value of heat temperature applied on bottom PVDF during the simulation. Heat temperature applied on top PVDF are fixed at 36 °C. Heat temperature difference is used as parameter to compare the power gained from the energy harvesting when constant force applied. 5 different heat temperature is applied to the bottom PVDF to compare the results of 50°C, 52°C, 54°C, 56°C and 58°C. The force of hot air flow applied in this simulation is fixed at 5N. Figure 4.8 shows the comparison graph on power output from theoretical and analytical calculation when different heat temperature is applied on bottom of PVDF.

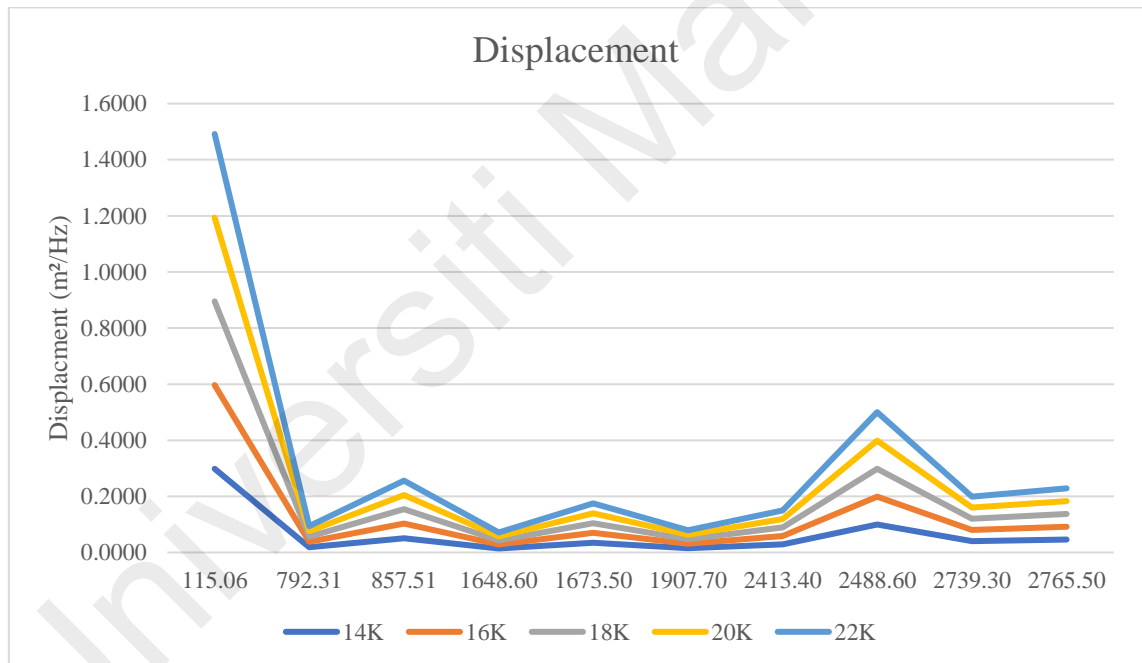
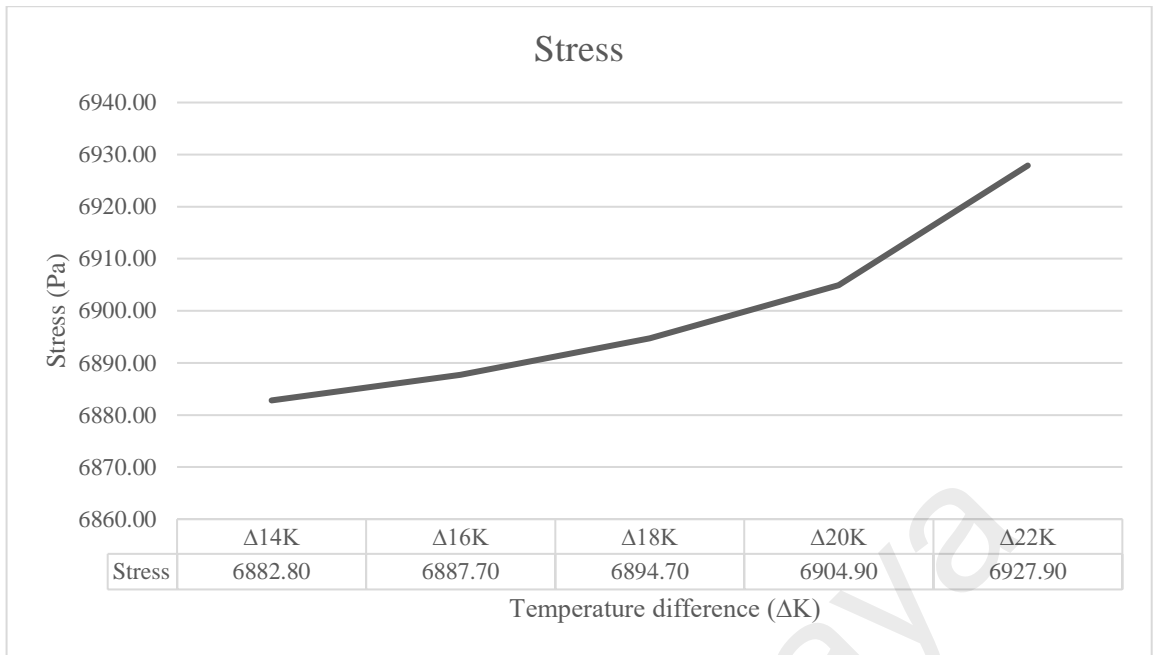
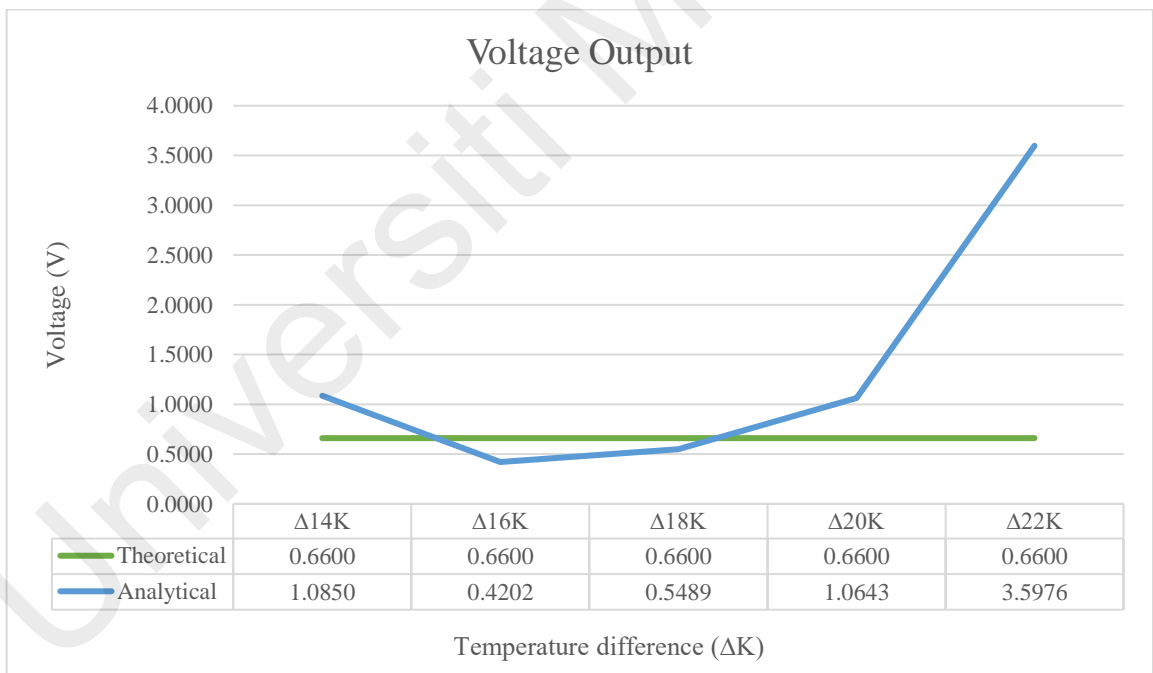


Figure 4.5: Heat temperature displacement



**Figure 4.6: Stress produce for heat temperature difference**



**Figure 4.7: Voltage output of temperature difference**

**Table 4.1: Piezoelectric power, pyroelectric power, and total power output**

Temperature difference ( $\Delta K$ )	Piezoelectric power (W)	Pyroelectric power(W)	Total Power Output (W)
14	1.5868E-07	3.7000E-03	3.7002E-03
16	2.3796E-08	4.2000E-03	4.2000E-03
18	4.0610E-08	4.3000E-03	4.3000E-03
20	1.5268E-07	4.7000E-03	4.7002E-03
22	1.7446E-06	5.1000E-03	5.1017E-03

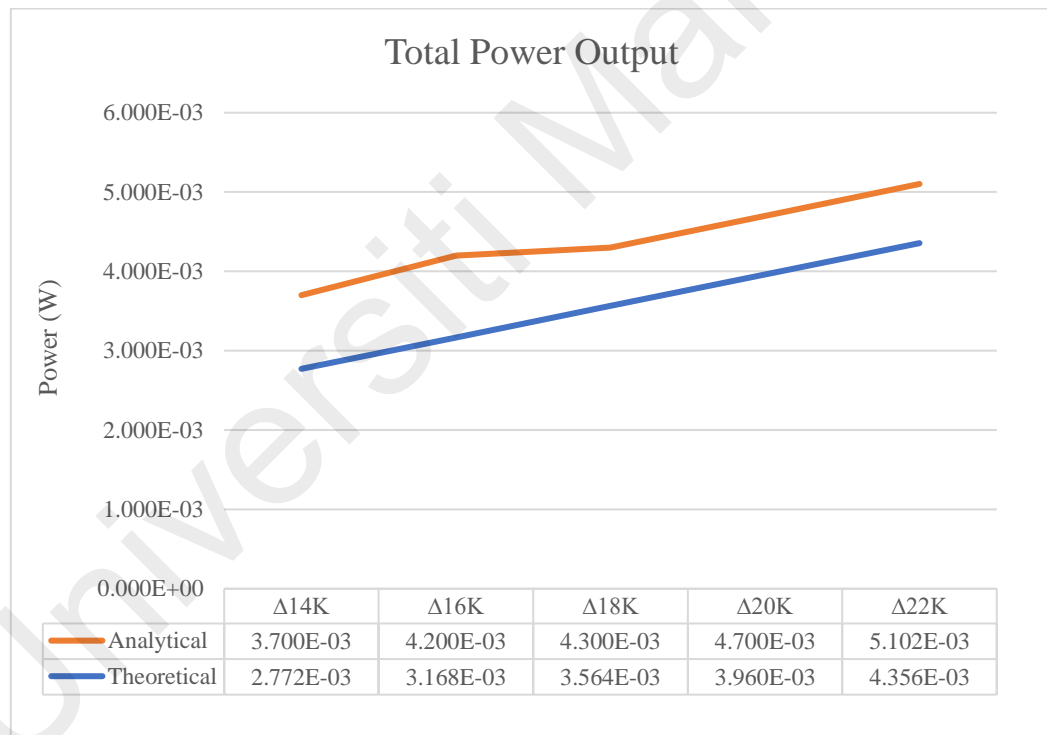


**Figure 4.8: Power output when difference temperature applied on bottom PVDF**

**Table 4.2: Error difference between theoretical and analytical power output**

<b>Temperature difference (<math>\Delta K</math>)</b>	<b>Theoretical (W)</b>	<b>Analytical (W)</b>	<b>Difference (%)</b>
14	2.7720E-03	3.7002E-03	25.00
16	3.1680E-03	4.2000E-03	24.57
18	3.5640E-03	4.3000E-03	17.11
20	3.9600E-03	4.7002E-03	15.75
22	4.3560E-03	5.1017E-03	14.62

**Table 4.3: Error difference between theoretical and analytical voltage output**

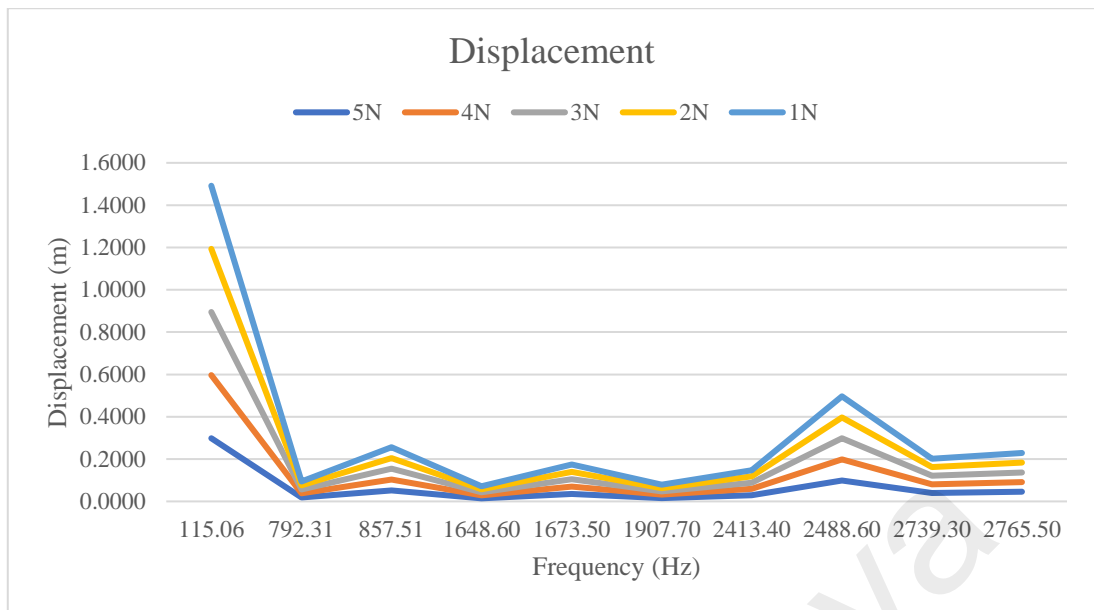
<b>Temperature difference (<math>\Delta K</math>)</b>	<b>Theoretical</b>	<b>Analytical</b>	<b>Difference (%)</b>
14	0.6600	1.0850	39.17
16	0.6600	0.4202	57.07
18	0.6600	0.5489	20.24
20	0.6600	1.0643	37.99
22	0.6600	3.5976	47.46

Figure 4.5 shows the displacement for every temperature difference parameter. From the graph,  $\Delta 22K$  produce the highest displacement value compared to another parameter. On the other hand, the highest displacement at frequency 115.06 Hz for every temperature difference parameter while the lowest displacement at 1648.60 Hz. Thus, the voltage output plot at frequency between 100 Hz until 130 Hz since highest displacement produce in that range of frequency. Based on figure 4.6, it shows the stress produce from the simulation of hybrid piezo-pyroelectric conversion device when different temperature is applied at constant force of 5N. From the graph it shows highest stress is at temperature difference  $\Delta 22K$  at 6927.90Pa while the lowest is at  $\Delta 14K$  at 6882.80Pa. Based on voltage

output graph on figure 4.7, for analytical calculation, it shows highest voltage produce is at  $\Delta 22\text{K}$  with  $3.60\text{V}$  and the lowest at  $\Delta 16\text{K}$  with  $0.42\text{V}$  whereas for theoretical calculation the voltage produce is same since the force applied is constant ( $5\text{N}$ ) which is  $0.66\text{V}$ . Table 4.1 shows the power produce from piezoelectric effect, pyroelectric effect, and total power output from both energy harvesting. Based on the graph on figure 4.8, it shows that for theoretical calculation, the power produce increases when higher temperature is applied for theoretical calculation. It shows that at  $\Delta 22\text{K}$  the power output produces at the highest with  $4.36\text{mW}$  while  $\Delta 14\text{K}$  produce the lowest power output  $2.77\text{mW}$ . For analytical, it shows the same result as theoretical. The highest power output produce is when temperature difference is  $\Delta 22\text{K}$  at  $5.10\text{mW}$  while the lowest at  $\Delta 14\text{K}$  with  $3.70\text{mW}$ . It can be concluded that power output for theoretical calculation is lower than analytical calculation. From the results, the heating effect the stress at certain point which then extend the stress in piezoelectric effect. Table 4.2 shows the different percentage from value of power output obtained from theoretical and analytical calculation. While on the contrary, table 4.3 shows the difference voltage output produce from analytical and theoretical calculation.

#### **4.2.2 Effect of different force applied on power performance**

This section focusing on different force applied when constant temperature and dimension is used. 5 different force is applied to get the results of power performance for both analytical calculation and theoretical calculation.  $1\text{N}$ ,  $2\text{N}$ ,  $3\text{N}$ ,  $4\text{N}$  and  $5\text{N}$  is applied to the device. Constant temperature and dimension are used for both calculations. Figure 4.8 shows the power output when different force is applied.



**Figure 4.9: Force displacement**

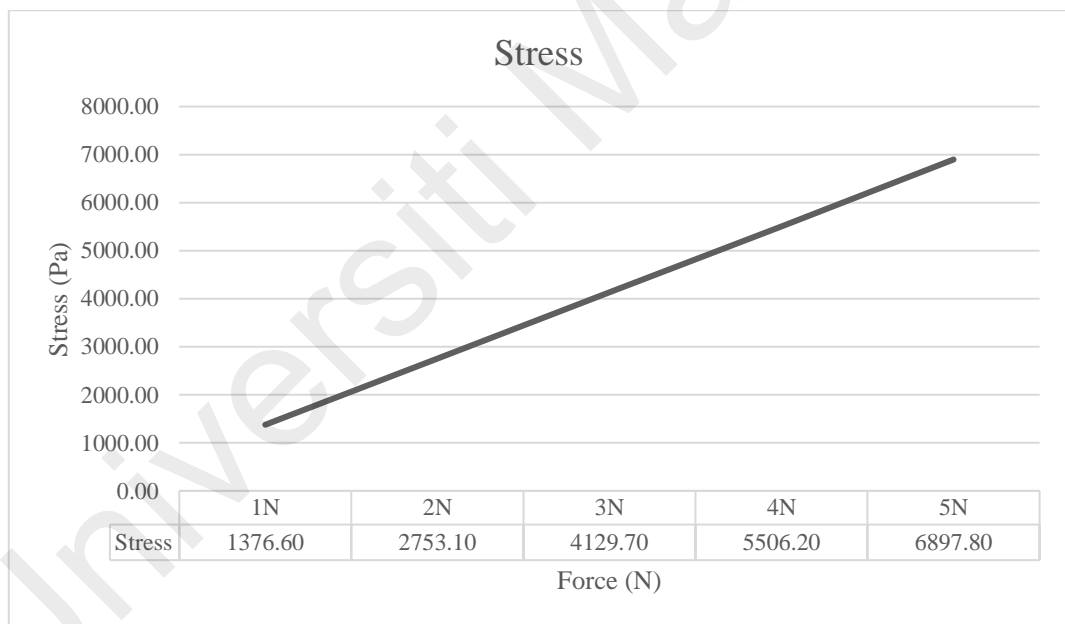


**Figure 4.10: Stress produce for different force applied**

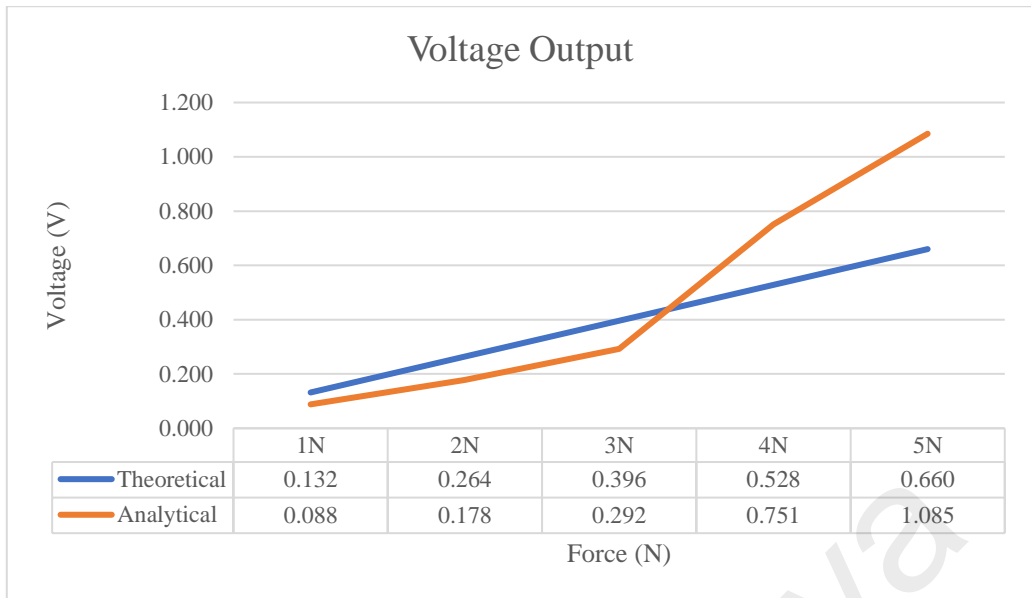


**Figure 4.11: Voltage output for force difference**

**Table 4.4: Piezoelectric power, pyroelectric power and the total power output**

Power (piezoelectric) (W)	Power (pyroelectric) (W)	Power Output (W)
2.135E-10	7.000E-04	7.000E-04
1.049E-10	1.400E-03	1.400E-03
9.019E-10	1.900E-03	1.900E-03
1.519E-08	2.500E-03	2.500E-03
1.587E-07	3.000E-03	3.000E-03

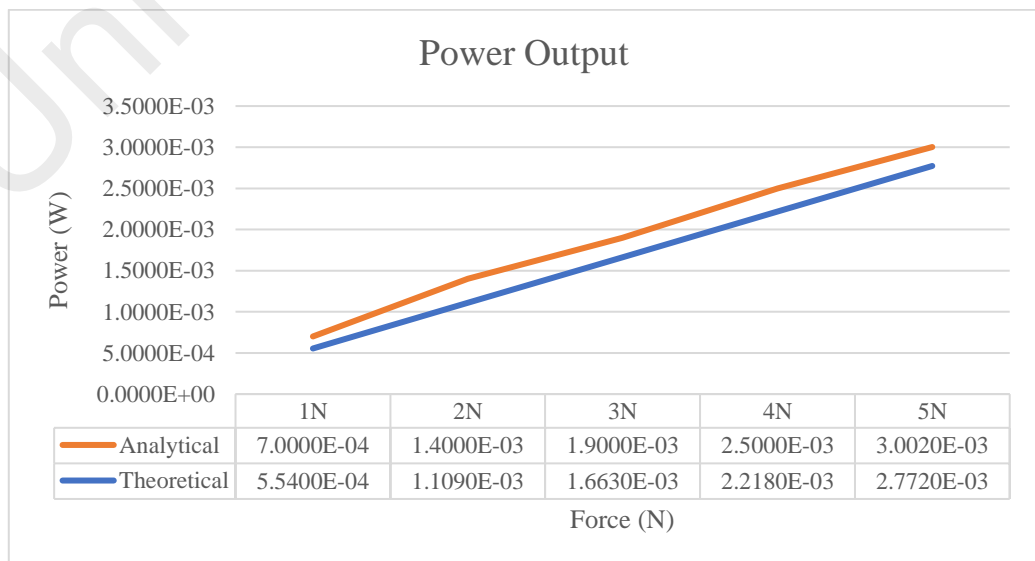


**Figure 4.12: Power output when different force is applied**

**Table 4.5: Error difference between theoretical and analytical power output**

Force (N)	Theoretical	Analytical	Difference (%)
1	0.554E-03	0.700E-03	20.86
2	1.109E-03	1.400E-03	20.79
3	1.663E-03	1.900E-03	12.47
4	2.218E-03	2.500E-03	11.28
5	2.772E-03	3.002E-03	7.66

**Table 4.6: Error difference between theoretical and analytical voltage output**

Force (N)	Theoretical	Analytical	Difference (%)
1	0.132	0.0890	32.58
2	0.264	0.178	48.31
3	0.396	0.211	46.67
4	0.528	0.751	29.66
5	0.660	1.085	39.17

The highest displacement produces in figure 4.9 at frequency 115.06 Hz and the lowest during frequency 1664.6 Hz. 1N force produce the highest displacement than other parameter for all frequency. Thus, the voltage output plotted graph is from 100 Hz to 130 Hz since the displacement produce at that frequency is the highest. The stress produces during simulation shown in figure 4.10 shows that highest stress produces at 5N with 6897.80Pa while the lowest is 1N with 1376.60Pa. The highest voltage produces when different force applied simulation is 1.085V when 5N force is applied during the simulation as shown in figure 4.11 whereas the lowest voltage output produce is at 1N with 0.089V. The highest voltage output produce from theoretical calculation is 0.66V when 5N is applied and the lowest is 0.132V when 1N is applied. Table 4.2 shows the

power produce from piezoelectric effect, pyroelectric effect and the total power output from both energy harvesting. From the graph in figure 4.12, it shows for theoretical calculation, the power output increases as higher force is applied. Highest power calculated is 2.77mW and the lowest is 0.55 mW whereas for analytical calculation, it shows that when 5N force is applied, power output is 3.0mW, which the highest power output and the lowest power output produce when 1N force is applied with 0.7mW. From the graph shows the power output for analytical calculation is higher than theoretical calculation. It also concludes that more force applied, higher stress and higher voltage produce thus more power output generate. Table 4.5 shows the difference of power output obtained for theoretical and analytical. While table 4.6 shows difference voltage output produce from analytical and theoretical calculation.

#### 4.2.3 Effect of different HDPE length on power performance

In this study, HDPE is use as the elastic material for the device. Figure 4.13 shows the power performance when different HDPE length is used with constant force applied of 5N and fixed temperature of 50°C is applied to the bottom PVDF.

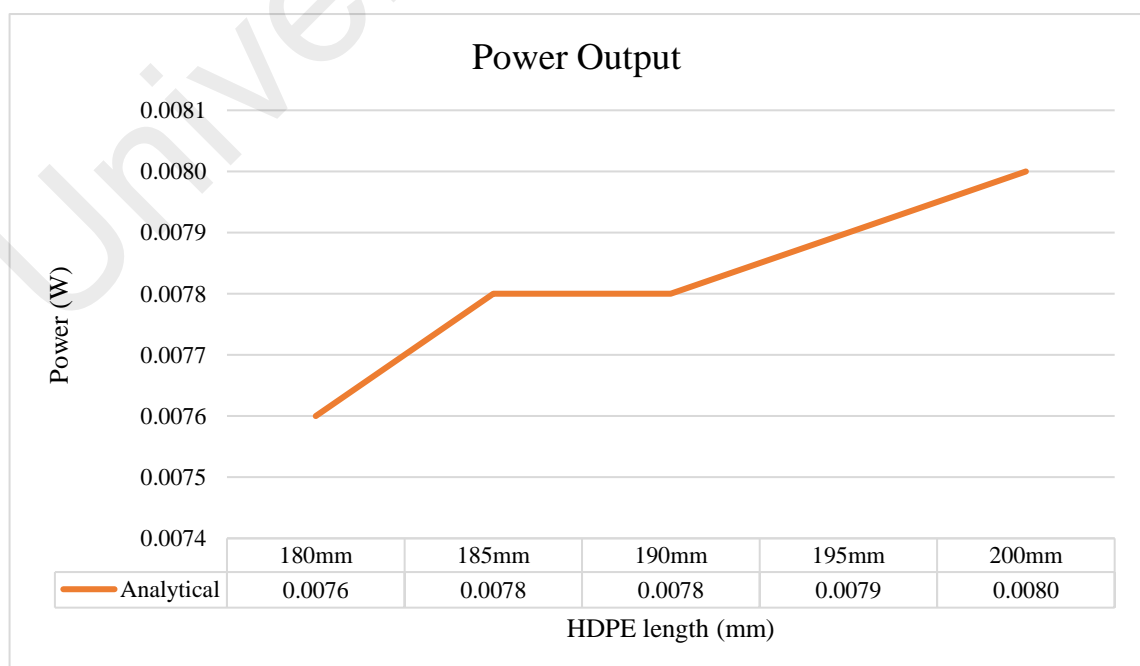


**Figure 4.13: Power output on different HDPE length**

Based on the graph, it shows that 200mm length of HDPE beam producing highest power than other length at 8mW. Figure 4.14 and figure 4.15 shows the deformation happen when 5N of force is applied to 180mm of HDPE length.

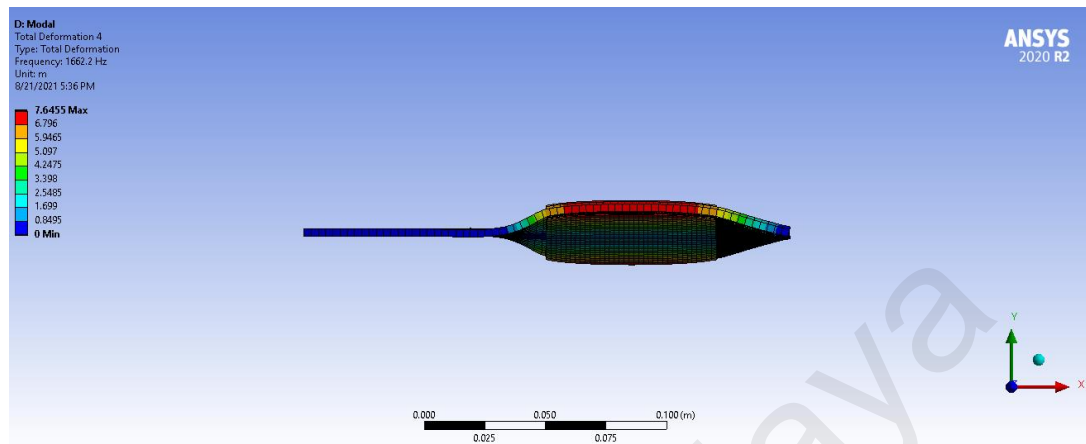


Figure 4.14: Total deformation 4

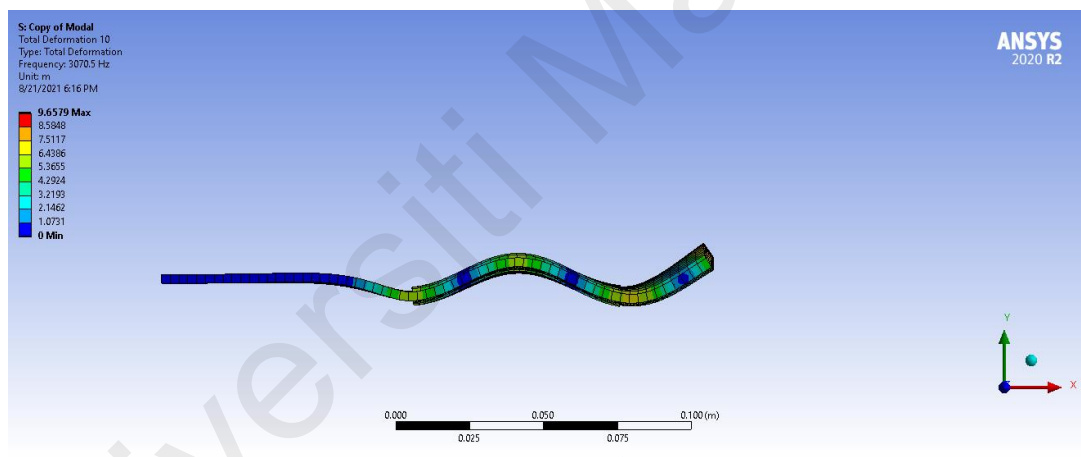
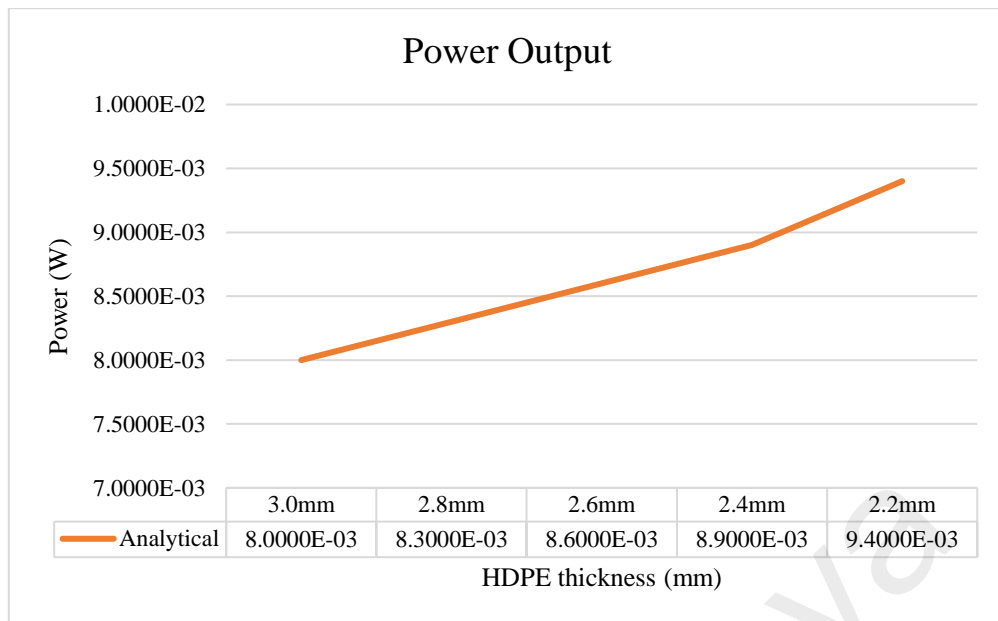


Figure 4.15: Total deformation 10

#### 4.2.4 Effect of different HDPE thickness on power performance

This section showing the effect of HDPE thickness on power performance. Figure 4.16 shows the graph on the effect of HDPE thickness on the power output with constant force 5N applied.



**Figure 4.16: Power output on different HDPE thickness**

Based on the graph produce on figure 4.16 for power output produce from different HDPE thickness when constant force and temperature of 5N and 50°C is applied to the bottom PVDF. This indicate the highest power output produce is during thickness 2.2mm of HDPE is 9.4mW while the lowest shows when 3.0mm HDPE thickness is used. From the graph shows that thinner HDPE produce more power output. Figure 4.16 and figure 4.17 shows the deformation happen during simulation of thickness 2.2mm.

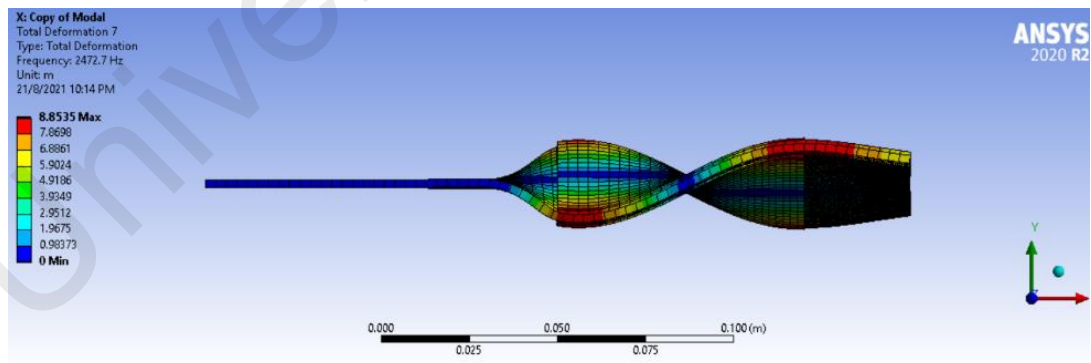


**Figure 4.17: Total deformation 7**

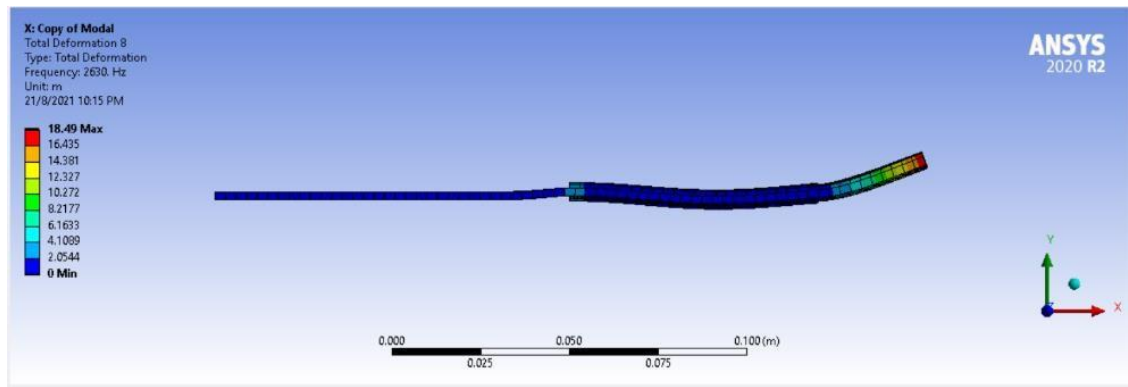


**Figure 4.18: Total deformation 8**

### 4.3 Discussion

The power performance results produce for parameter temperature and force are discussed to state the reason why there is difference in the power output for theoretical calculation and analytical calculation. From the voltage over frequency graph, it can be seen that the voltage produces when difference force applied is higher than when different temperature applied. This is due to maximum force is applied since piezoelectricity is affected by the mechanical stress applied.

As shown for temperature and force difference graph, power produce from analytical calculation is bigger than theoretical calculation. This can be stated that analytical calculation based on real behavior of the device under test with specific parameter. While theoretical calculation is made from series of assumptions to develop a model. Simulation considering more parameter than theoretical calculation. Simulation involves development of model, mathematical equation model for the device and solving system of equations and post processing step to get performance of the device based on the parameter used. During solving system of equations and post-processing stage, the results can be verified. This can be concluded that simulation modelling solves real-life problems and analyze the result efficiently while theoretical calculation can be said as assumption to compare the result.

As demonstrated, from the power output produce from force applied, it shows that highest analytical power output produce is 3.0mW when the force applied is 5N and for theoretical power output is 2.77mW. It also shown in figure 4.11 that when force applied increases, the stress produces increases. Piezoelectric energy depends on stress produce in between piezoelectric material. Since piezoelectric effect is response to mechanical stress when pressure is applied, thus force applied give effect to the piezoelectric since  $P = F/A$ . From the formula, we can make conclusion pressure produce during 5N force applied is high, thus more electricity produces thus more power output created.

For different temperature applied on bottom PVDF, it shows that the highest analytical power output produce is 5.10mW and for theoretical is 1.09mW when the 58°C of hot air is applied at the bottom PVDF. This can be concluded that during that condition, the crystal of piezoelectric material is at peak then causes the atom from neutral position hence it exhibits spontaneous polarization of piezoelectric material and produce higher power output.

According to (Covaci & Gontean, 2020) maximum power output produce from dimension 72mm x 16mm x 0.41mm is 0.61mW at 2 Hz frequency. This previous study can validate the analytical power produce in this study since the dimension used is bigger and power output generate higher. As indicated in study by (Hu & Tao, 2016) stated when 25.4mm x 25.4mm PVDF is used to harvest hybrid piezo-pyroelectric energy, maximum voltage generate is 70mV when 60°C heat is applied and mechanical loading with weight of 31.7g is used. Another study by (Xie et al., 2010) stated that PVDF area of 1.96cm<sup>2</sup> and thickness of 110µm producing 0.49V of measured voltage and 0.53V predicted peak voltage when 30°C until 141°C temperature is used. Meanwhile for peak power output generate is 0.24mW for measured and 0.26mW for predicted value. (Kundu & Nemade, 2016) stated that harvested power of 0.323mW is generate when optimal load resistance at 10.3kΩ and displacement end mass is 127µm. Since dimension of PVDF used in this

study much smaller than used in study by (Kundu & Nemade, 2016) thus the power output produce from theoretical calculation are valid. As mentioned by (Hu & Tao, 2016) pure PVDF material generate lower energy than other piezoelectric material such as PZT and PVDF nanocomposites since the piezoelectric coefficient of the material is lower than others. From all previous research work can be summarized maximum theoretical and analytical power output produce with the dimension PVDF of 100mm x 50mm x 1mm is valid. Since PVDF has low piezoelectric coefficient thus it required bigger dimension to harvest same value power output as PZT.

From the comparison between force and temperature power output, it indicated that power output produces from temperature difference generate higher value than different force applied. This shows that pyroelectric effect does enhancing the hybrid piezo-pyroelectric power produce from the device. (Kang & Yeatman, 2016) also stated that pyroelectric effect does enhance the piezoelectric output by using different temperature with fixed mechanical stops. From table 4.1 and table 4.2 shows power produce from piezoelectric effect lower than power produce from pyroelectric effect. This indicate that pyroelectric effect does give huge impact during hybrid piezo-pyroelectric energy harvesting.

For HDPE length, it shows that the highest power output is when the length is 200mm. This shows that the most suitable length to gain more power output is by using HDPE with length of 200mm. While for the HDPE thickness, it shows that 2.2mm produce highest power output than others. So, the suitable device elastic support dimension can be used is 200mm x 2.2mm.

Furthermore, from table 4.2, 4.3, 4.5 and 4.6 shows the error difference for voltage output and total power output for both analytical and theoretical value. This error can be assumed produce from the parameter applied during simulation. Since there is no parameter such as air velocity is assumed during theoretical calculation thus the value

calculated will be different from simulation. (Xie et al., 2010) indicated in their study the difference percentage of peak voltage and peak power produced from measured and predicted value. For PVDF material, it stated that the difference between measured and predicted value for peak voltage is 8% while for peak power also 8%. Some of the error difference for theoretical and analytical in this study is unacceptable such as highest difference value for voltage which is 57% since the percentage close to zero or below 10% is considered as a good result and below 30% is acceptable. Above the percentage, the error is unacceptable. To reduce this error, some preventive can be done. Firstly, by double checking the material data used for copper, PVDF and HDPE material inside engineering data. Secondly, ensure all vital parameter had been applied.

Universiti Malaya

## CHAPTER 5

### CONCLUSION AND RECOMMENDATION

#### 5.1 Conclusion

Hybrid piezo-pyroelectricity is known as an important sustainable energy since the energy sources can easily find. The power output produce from the device can be different due to the parameter applied on the piezoelectric material. Piezoelectric is known as electric charge generate inside crystal from the response of mechanical stress when it is squeeze or pressed. While piezoelectricity is generation of electrical potential or known as voltage across the crystal. So usually, this energy can only be harvest when there is force or pressure applied on the piezoelectric material. Pyroelectric is defined as generation of voltage or current when there is thermal condition whether it is heated or cooled. Thus, in this study, the generation of voltage when the piezoelectric material is heated, and force applied to create vibration on the device.

The objective of this study is to design a hybrid piezo-pyroelectric energy scavenging device for low heat grade applications were achieved. The design of the device is shown in subchapter 3.7.1. The device succeeds to produce power output as shown table 5.1. Secondly, the theoretical and analytical calculation of the power output were done and shown in chapter 3 and 4 in results section. All calculation for voltage output, piezoelectric energy, pyroelectric energy, and total power output produce are calculated. Lastly, the hybrid piezo-pyroelectric energy scavenging device simulation were succeeded model and run, and the performance of the device are shown in chapter 4 results section. The performance of the device included stress, voltage output and total power output produce by the model from the simulation run.

To power up a temperature sensor with 20mW, number of devices needed to ensure sufficient power is supply. Table 5.1 showing the number if device needed based on the maximum power produce:

**Table 5.1: Number of devices needed**

Parameter	Maximum Power output	Number of devices needed
Temperature - Theoretical	2.77mW	8
Temperature - Analytical	4.36mW	5
Force - Theoretical	0.70mW	29
Force - Analytical	3.00mW	7

From all the results and discussions made on chapter 4, it shows that analytical calculation is higher than theoretical calculation for voltage output and total power output for force difference and temperature difference parameter. Other than that, the temperature difference parameter produces higher total power output and voltage output than force difference parameter. From the table 3.5 and 3.6 for theoretical calculation, it shows that pyroelectric produce higher charge than piezoelectric. This trend also can be seen on table 4.1 and 4.4, it shows that piezoelectric power produce is lower than pyroelectric. This can be concluded that pyroelectric effect plays a huge role in hybrid piezo-pyroelectric effect.

As conclusion, all three objectives were achieved. From the methodology to run the simulation, the data gained succeeded to achieve the objectives. In this study also shows that pyroelectric effect enhanced the piezoelectric voltage output when it is using different temperatures since it increases the pressure produce. The effect on different force applied to create mechanical vibration shown to be increases as more stress and pressure produce.

## 5.2 Recommendation

There are a several recommendations that can be made to improve this study. The recommendations are:

- 1) Improve the dimension of the design to get more power output produce. This can be done by change the HDPE dimension based on the simulation done on the performance of HDPE thickness and length when constant force is applied.
- 2) Used another design other than cantilever. As shown in subchapter 2.5, there are other design can be used to harvest the hybrid piezo-pyroelectric energy.
- 3) Electrode size can be change and test to find out the suitable size to increase the device performance Based on study by (Fu et al., 2018) indicate output voltage increases with decreases electrode coverage ratio. Hence, the performance of harvester can be improved by designing optimized electrode.

## References

- Academy, D. C. (2021). *Introduction to CAD*.  
<https://www.designtechcadacademy.com/knowledge-base/introduction-to-cad>
- ANSYS, I. (2010). ANSYS Multiphysics Solutions. In.
- Arevalo Carreno, A. A., & Foulds, I. (2013). *Parametric Study of Polyimide – Lead Zirconate Titanate Thin Film Cantilevers for Transducer Applications*.
- Bowen, C., Xie, M., Zhang, Y., Topolov, V., & Wan, C. (2018). Pyroelectric Energy Harvesting: Materials and Applications. In (pp. 203-229).  
<https://doi.org/10.1002/9783527807505.ch7>
- Caliò, R., Rongala, U., Camboni, D., Milazzo, M., Stefanini, C., De Petris, G., & Oddo, C. (2014). Piezoelectric Energy Harvesting Solutions. *Sensors (Basel, Switzerland)*, *14*, 4755-4790. <https://doi.org/10.3390/s140304755>
- Covaci, C., & Gontean, A. (2020). Piezoelectric Energy Harvesting Solutions: A Review. *Sensors*, *20*, 3512. <https://doi.org/10.3390/s20123512>
- Dudhat, P., Li, Q., & Ren, S. (2019). ANSYS Simulation of Piezoelectric Patch for Energy Harvesting.
- E, V., & Rajakumar, S. (2018). Performance improvement of piezoelectric materials in energy harvesting in recent days – A review. *Journal of Vibroengineering*, *20*.  
<https://doi.org/10.21595/jve.2018.19434>
- Fu, H., Chen, G., & Bai, N. (2018). Electrode Coverage Optimization for Piezoelectric Energy Harvesting from Tip Excitation. *Sensors*, *18*, 804.  
<https://doi.org/10.3390/s18030804>
- Ghazanfarian, J., & Mohammadi, M. (2021). *Piezoelectric Energy Harvesting: a Systematic Review of Reviews*.
- Haider, J., Salleh, H., Supeni, E. E., As'array, A., Md Rezali, K. A., & Atrah, A. (2020). Harvesting Energy from Planetary Gear Using Piezoelectric Material. *Energies*, *13*, 223. <https://doi.org/10.3390/en13010223>
- Hu, J., & Tao, J. (2016). Energy Harvesting from Pavement via PVDF: Hybrid Piezo-Pyroelectric Effects. In *Geo-Chicago 2016* (pp. 556-566).  
<https://doi.org/doi:10.1061/9780784480137.053>
- Kang, M., & Yeatman, E. (2016). Thermal Energy Harvesting Using Pyroelectric and Piezoelectric Effect. *Journal of Physics: Conference Series*, *773*, 012073.  
<https://doi.org/10.1088/1742-6596/773/1/012073>
- Kim, S., Park, H., Kim, S., Wickle, H. C., Park, J., & Kim, D. (2013). Comparison of MEMS PZT Cantilevers Based on  $\text{d}_{31}$  and  $\text{d}_{33}$  Modes for Vibration Energy Harvesting. *Journal of Microelectromechanical Systems*, *22*(1), 26-33.  
<https://doi.org/10.1109/JMEMS.2012.2213069>

- Koyuncuoglu, A., Özyurt, O., Okutucu, T., Kulah, H., & Zorlu, Ö. (2013). *Hybrid Energy Harvester Using Piezoelectric and Pyroelectric Properties of PZT-5A Ceramics*. <https://doi.org/10.2514/6.2013-4030>
- Kundu, S., & Nemade, H. B. (2016). Modeling and Simulation of a Piezoelectric Vibration Energy Harvester. *Procedia Engineering*, 144, 568-575. <https://doi.org/https://doi.org/10.1016/j.proeng.2016.05.043>
- Pandya, S., Velarde, G., Zhang, L., Wilbur, J., Smith, A., Hanrahan, B., Dames, C., & Martin, L. (2019). New approach to waste-heat energy harvesting: pyroelectric energy conversion. *NPG Asia Materials*, 11, 26. <https://doi.org/10.1038/s41427-019-0125-y>
- Poh, W. Q. T., Muhammad Ramadan, B. M. S., & Logenthiran, T. (2018). *Design and Simulation of a Piezoelectric Cantilever Beam for Mechanical Vibration Energy Harvesting*. <https://doi.org/10.1109/ISGT-Asia.2018.8467796>
- Safaei, M., Sodano, H. A., & Anton, S. R. (2019). A review of energy harvesting using piezoelectric materials: state-of-the-art a decade later (2008–2018). *Smart Materials and Structures*, 28(11), 113001. <https://doi.org/10.1088/1361-665x/ab36e4>
- Sezer, N., & Koç, M. (2021). A comprehensive review on the state-of-the-art of piezoelectric energy harvesting. *Nano Energy*, 80, 105567. <https://doi.org/https://doi.org/10.1016/j.nanoen.2020.105567>
- Shashank, R., Harisha, S., & Abhishek, M. (2018). Modelling and analysis of piezoelectric cantilever energy harvester for different proof mass and material proportion. *IOP Conference Series: Materials Science and Engineering*, 310, 012147. <https://doi.org/10.1088/1757-899X/310/1/012147>
- Tao, J., & Hu, J. (2016). Energy harvesting from pavement via polyvinylidene fluoride: hybrid piezo-pyroelectric effects. *Journal of Zhejiang University-SCIENCE A*, 17(7), 502-511. <https://doi.org/10.1631/jzus.A1600166>
- Thakre, A., Kumar, A., Song, H.-C., Jeong, D.-Y., & Ryu, J. (2019). Pyroelectric Energy Conversion and Its Applications—Flexible Energy Harvesters and Sensors. *Sensors*, 19(9). <https://doi.org/10.3390/s19092170>
- Triani, R. Pyroelectricity.
- Xie, J., Mane, X. P., Green, C., Mossi, K., & Leang, K. (2010). Performance of Thin Piezoelectric Materials for Pyroelectric Energy Harvesting. *Journal of Intelligent Material Systems and Structures - J INTEL MAT SYST STRUCT*, 21. <https://doi.org/10.1177/1045389X09352818>
- Yaakub, M., Basar, M., Noh, F. H., & Kamarudin, H. Z. (2017). A micro-power generation from rain shower utilizing PZT and PVDT piezoelectric transducer. *ARPJ Journal of Engineering and Applied Sciences*, 12, 6285-6290.

Yildiz, F., Dakeev, U., Baltaci, K., & Coogler, K. (2015). Energy harvesting from air conditioning condensers with the use of piezoelectric devices. *ASEE Annual Conference and Exposition, Conference Proceedings*, 122.

Zeid, I. (2004). *Mastering Cad Cam*. MCGRAW HILL COMPANIES.

Zi, Y., Lin, L., Wang, J., Wang, S., Chen, J., Fan, X., Yang, P.-K., Yi, F., & Wang, Z. L. (2015). Triboelectric–Pyroelectric–Piezoelectric Hybrid Cell for High-Efficiency Energy-Harvesting and Self-Powered Sensing. *Advanced Materials*, 27(14), 2340-2347. <https://doi.org/https://doi.org/10.1002/adma.201500121>

Universiti Malaya